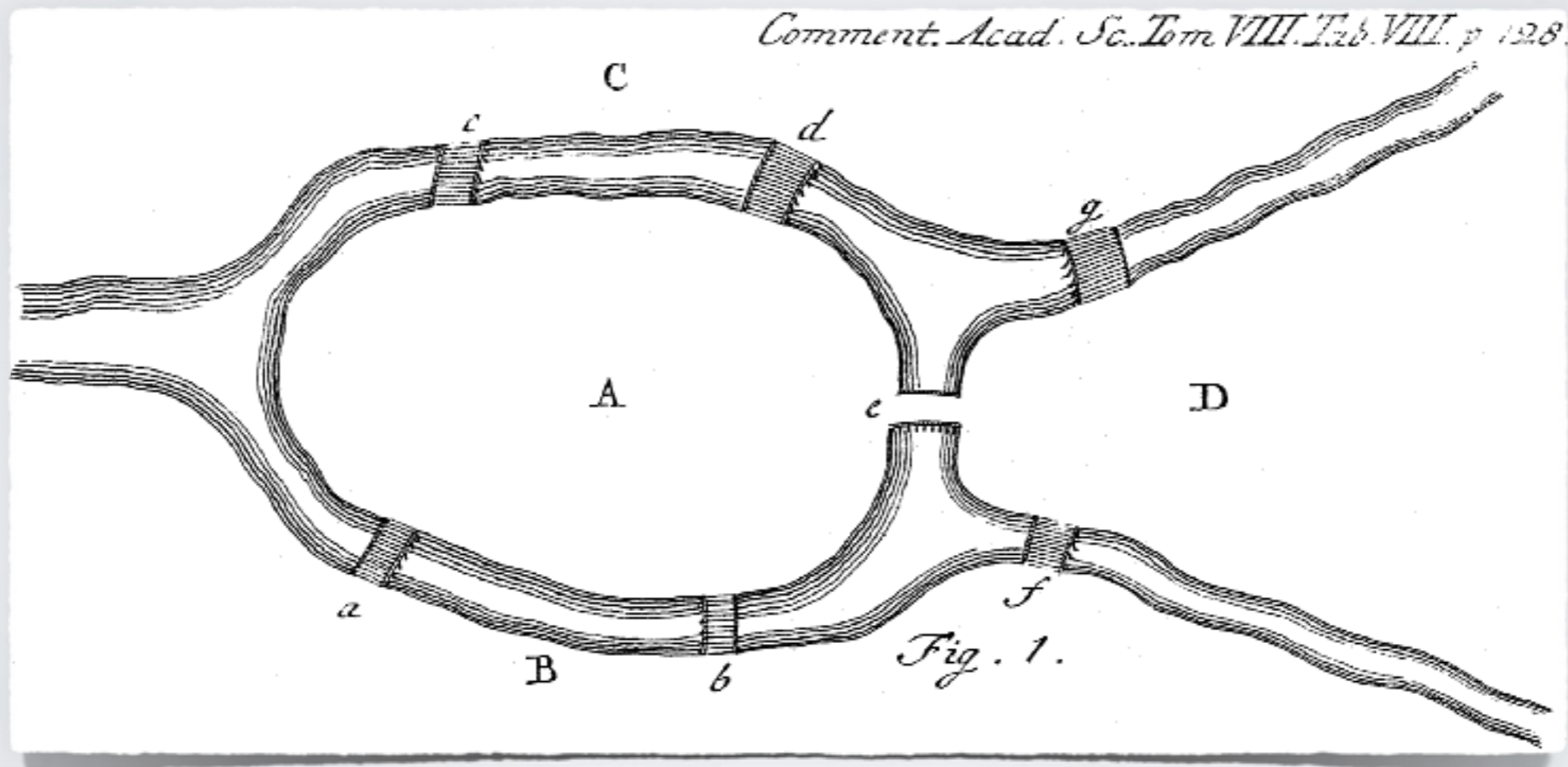


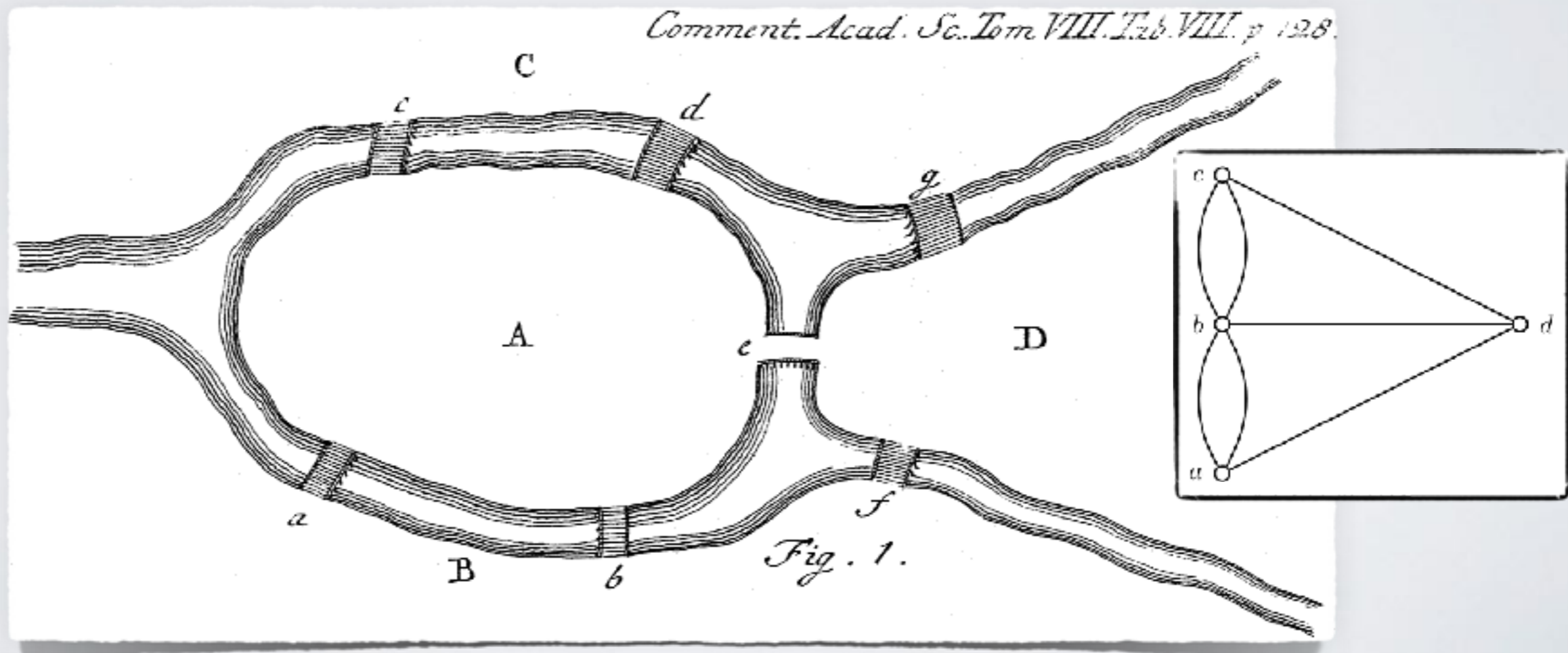
URBAN MOBILITY NETWORKS

Seven Bridges of Königsberg



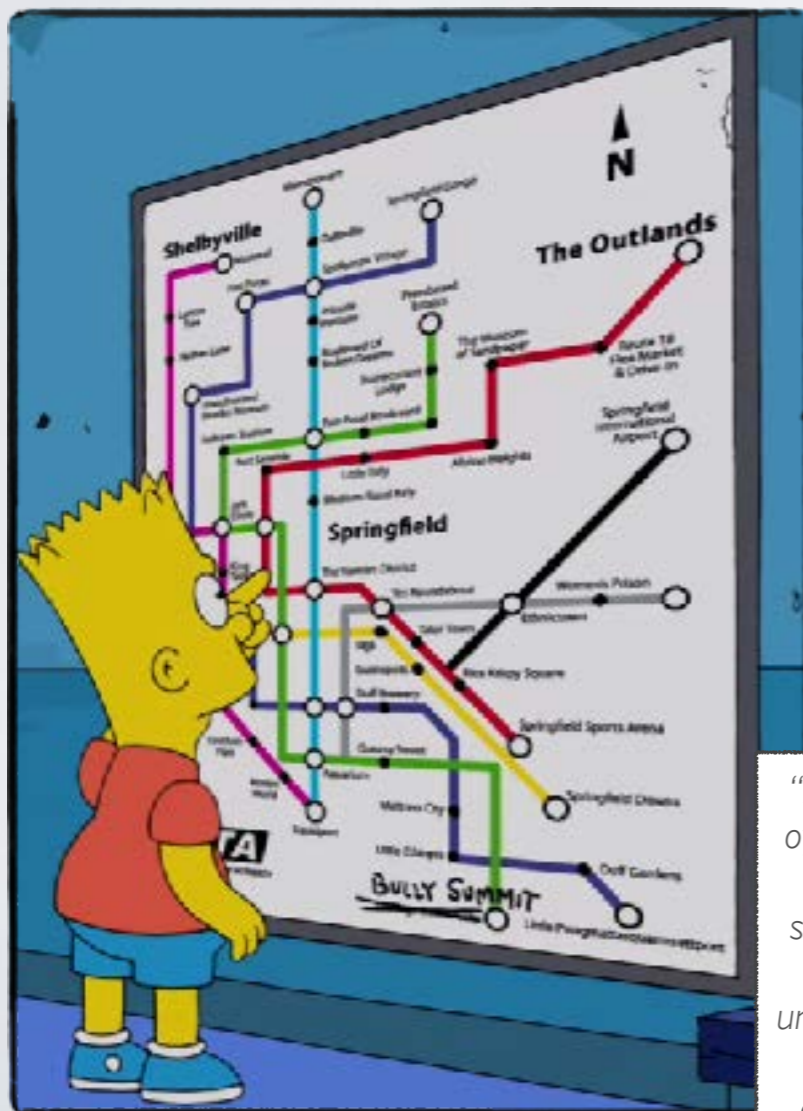
URBAN MOBILITY NETWORKS

Seven Bridges of Königsberg



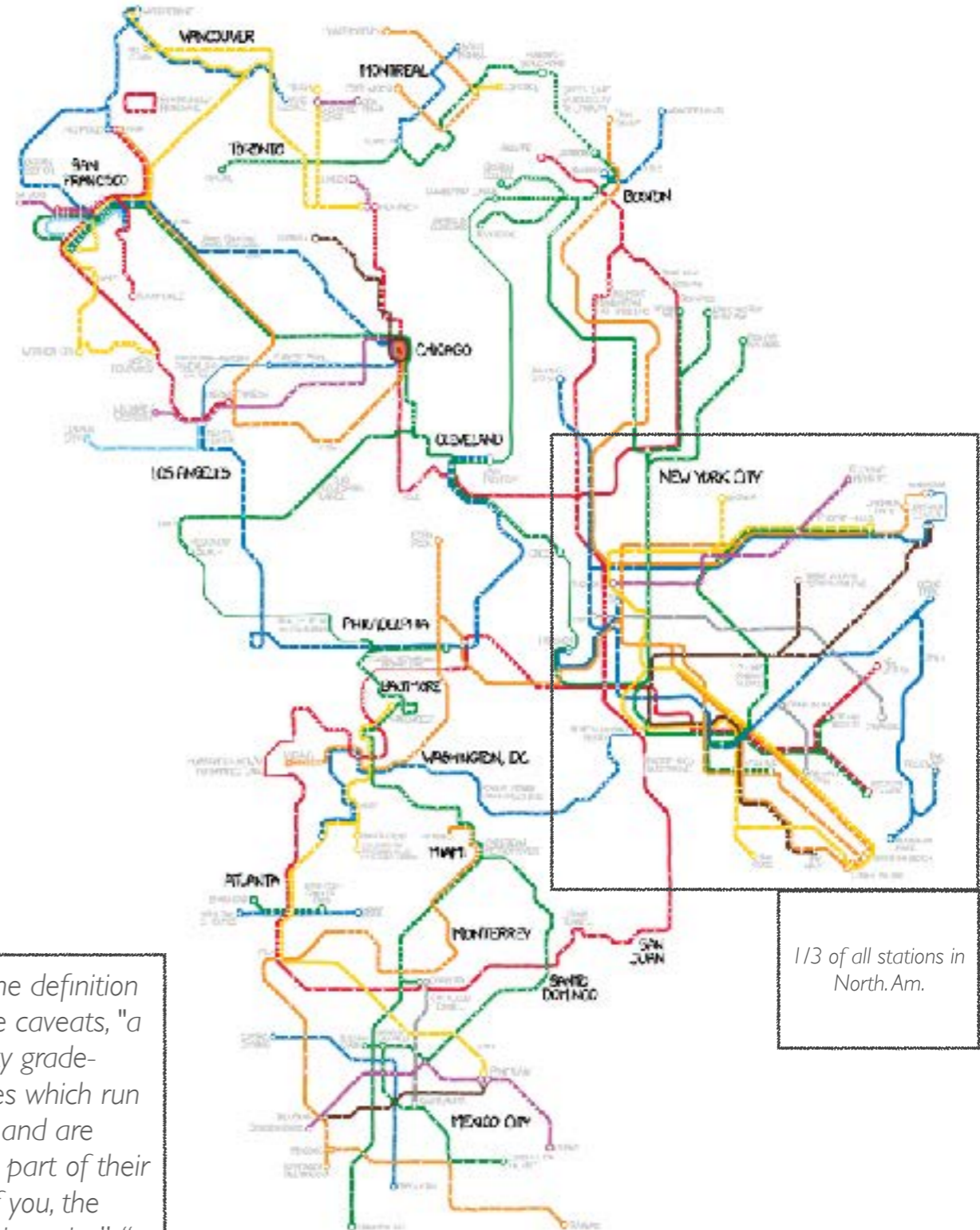
SPATIAL NETWORKS

- **Various types:**
 - *Real transport networks*



"For the pedantic rail enthusiasts, the definition of a subway used here is, with some caveats, "a network containing high capacity grade-separated passenger rail transit lines which run frequently, serve an urban core, and are underground or elevated for at least part of their downtown route." For the rest of you, the definition is "an underground train in a city." "

SUBWAYS OF NORTH AMERICA



1/3 of all stations in North Am.

SPATIAL NETWORKS

- **Various types:**

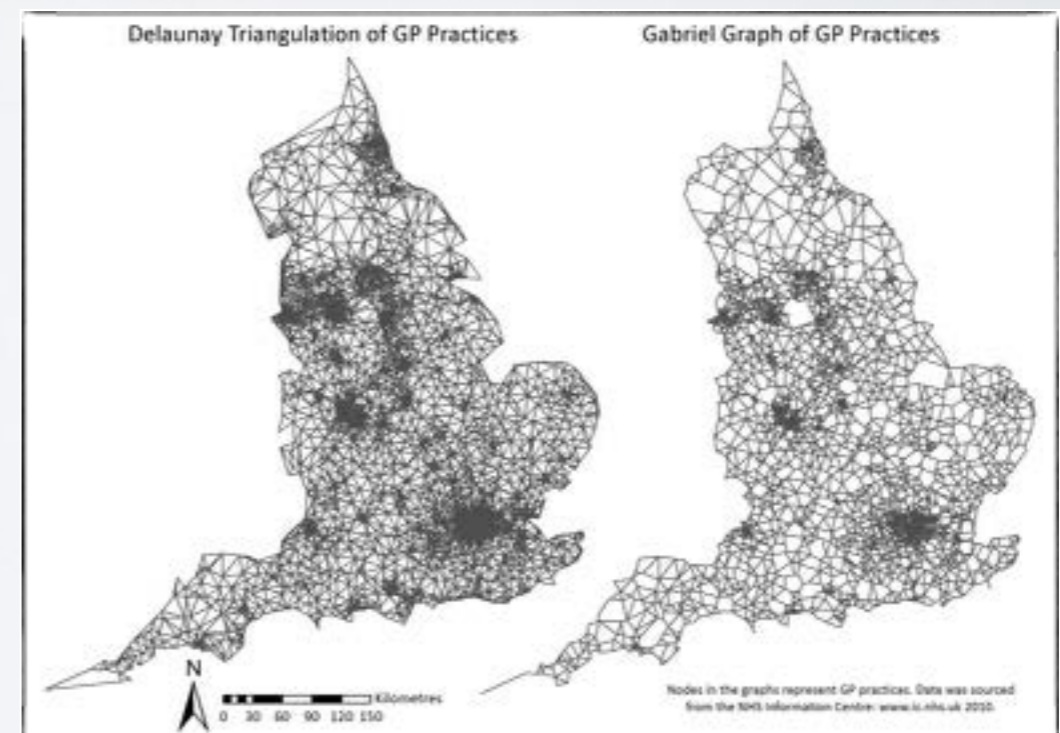
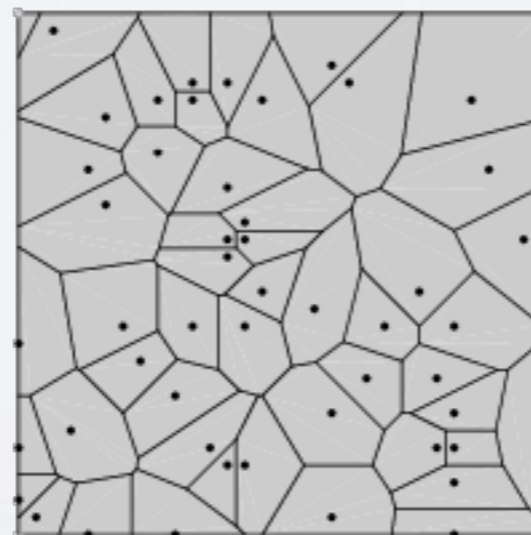
- *Real transport networks*

- *Mobility networks*

- between fixed nodes

- or indetermined nodes

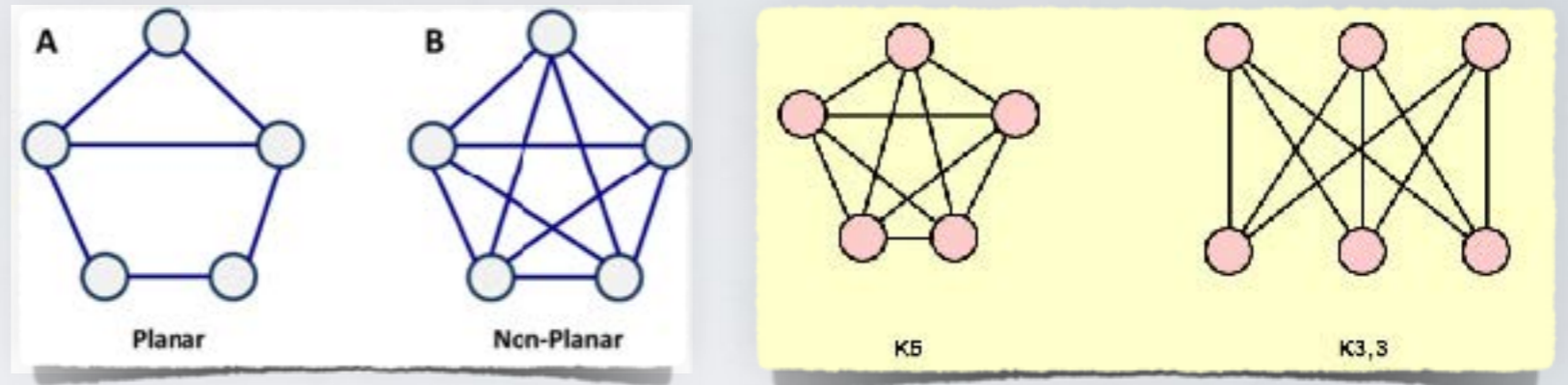
- *Voronoi paving*



SPATIAL NETWORKS

- **Various structures:**

- Most are planar
- Representations may vary



- e.g. “station space” vs. “stop space”

- **Distinct from other types of networks,** especially social networks

- Connectivity related to transfert
 - strongly bounded (often 2)
- Small clustering

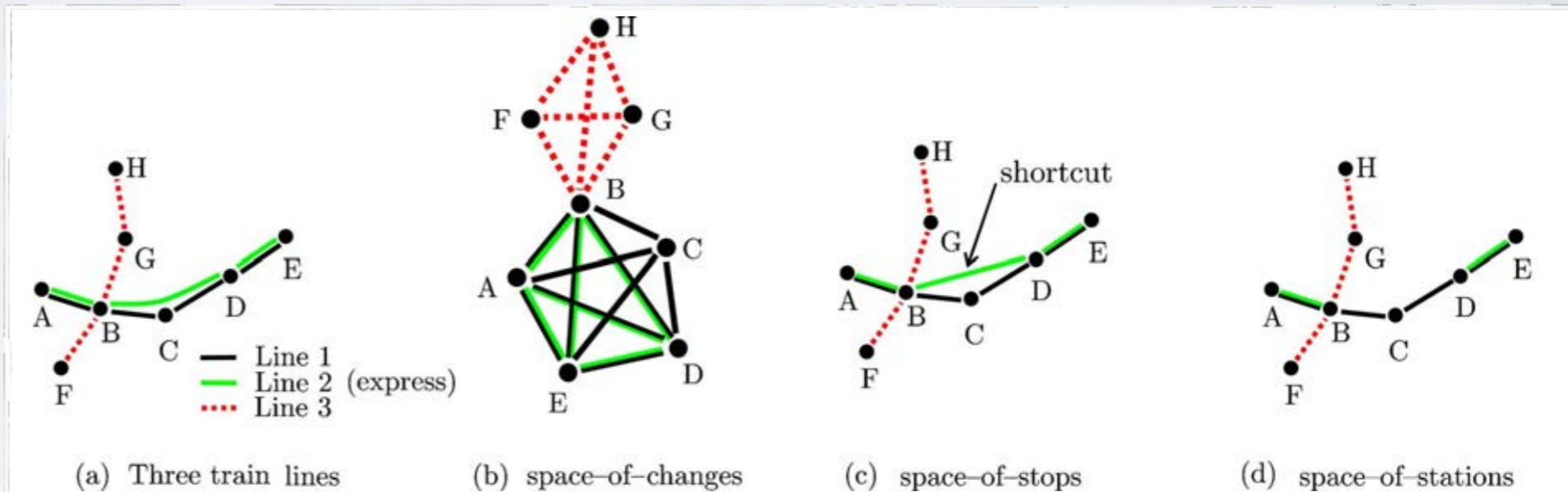
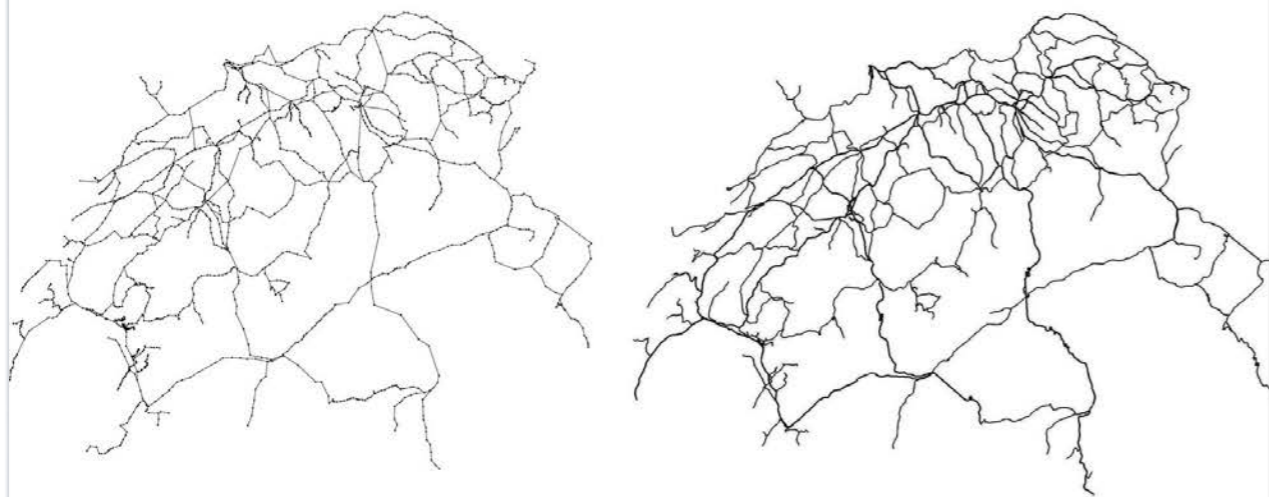
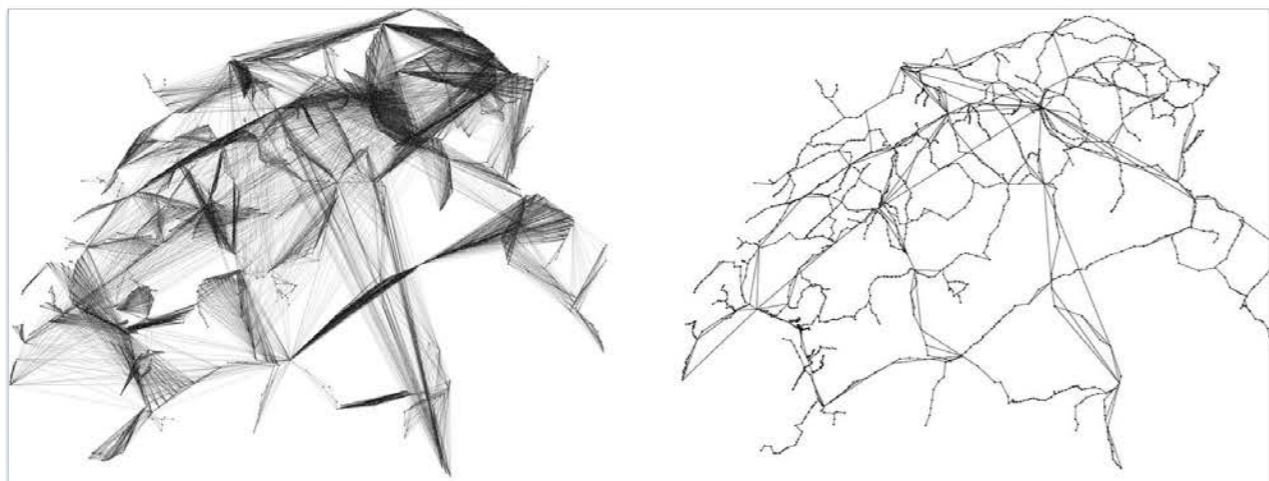


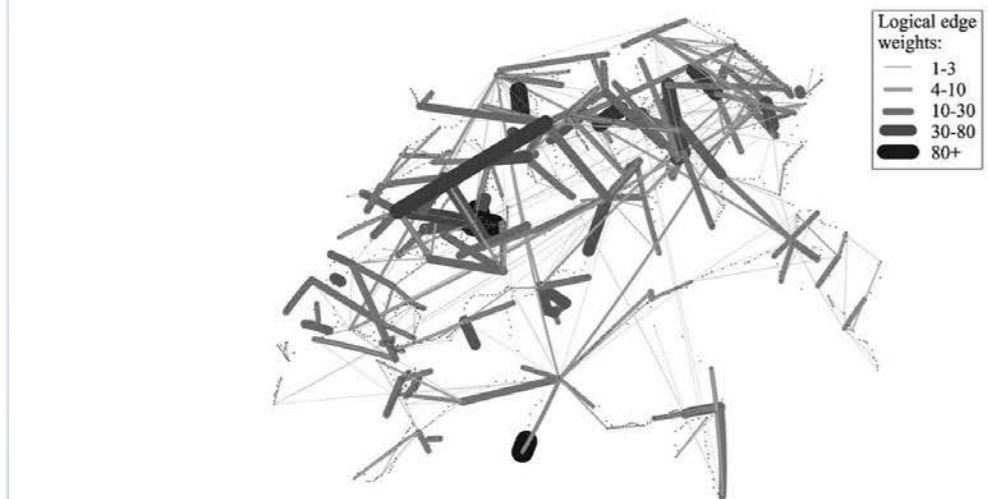
FIG. 1. (Color online) An illustration of the transportation network topology in three spaces. (a) The routes of three vehicles. The route of line 2 passes through node C on the way from B to D , but the vehicle does not stop there. (b) The topology in the space of changes. Each route results in a clique. An edge is indicated by two colors, when it originates from two routes, but is merged into a single link. (c) The topology in the space of stops. The “shortcut” $B-D$ is a legitimate edge in this space. (d) The topology in the space of stations. This graph reflects the topology of the real-life infrastructure.

(Kurrant, Thiran, 2006)

(Kurrant, Thiran, 2006)



(a) Physical graph G_{change}^ϕ in space-of-changes (b) Physical graph G_{stop}^ϕ in space-of-stops



(e) Logical graph

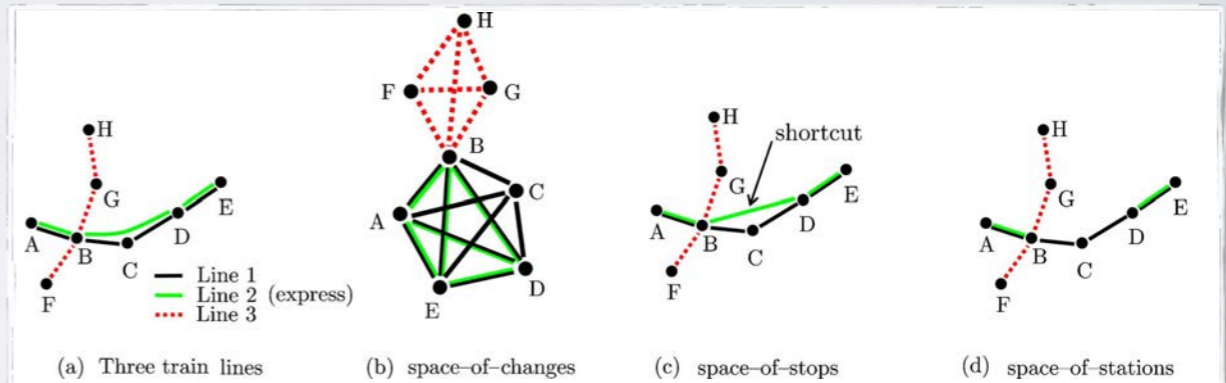


FIG. 1. (Color online) An illustration of the transportation network topology in three spaces. (a) The routes of three vehicles. The route of line 2 passes through node C on the way from B to D , but the vehicle does not stop there. (b) The topology in the space of changes. Each route results in a clique. An edge is indicated by two colors, when it originates from two routes, but is merged into a single link. (c) The topology in the space of stops. The "shortcut" $B-D$ is a legitimate edge in this space. (d) The topology in the space of stations. This graph reflects the topology of the real-life infrastructure.

FIG. 3. The railway network in Switzerland (CH). (a), (b), (c) Physical graphs in the space of changes, stops, and stations, respectively. (d) The real map of the rail tracks in Switzerland. (e) The logical graph. Every edge connects the first and last stations of a particular train route; its weight reflects the number of trains following this route in any direction.

SPATIAL NETWORKS



Betweenness centrality for the road network of Dresden, Saxony

HUMAN MOBILITY

Mobile phones



From mobile phone data to the spatial structure of cities

Thomas Louail^{1,2}, Maxime Lenormand³, Oliva G. Cantu Ros⁴, Miguel Picornell⁴, Ricardo Herranz⁴, Enrique Frias-Martinez⁵, José J. Ramasco³ & Marc Barthelemy^{1,6}

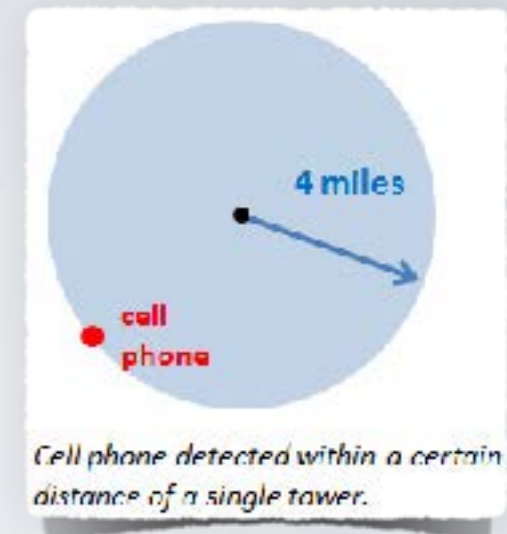


Figure 1 | The 31 Spanish urban areas with more than 200,000 inhabitants in 2011. Map of their locations and spatial extensions.

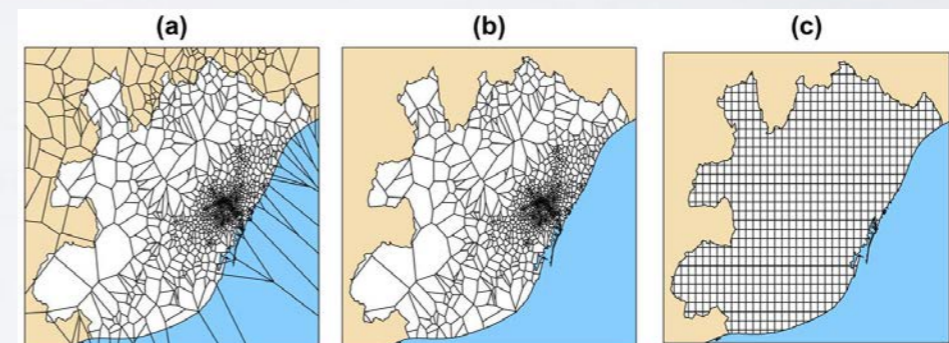
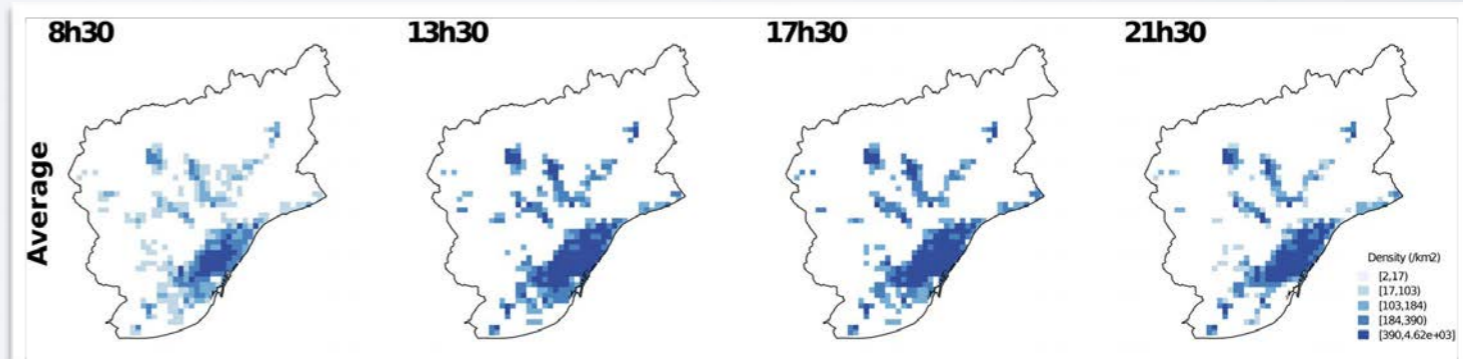


Figure 3 | Map of the metropolitan area of Barcelona. The white area represents the metropolitan area (administrative delimitation), the brown area represents territories surrounding the metropolitan area and the blue area the sea. (a) Voronoi cells of the mobile phone antennas point pattern. (b) Intersection between the Voronoi cells and the metropolitan area. (c) Grid composed of 1 km² square cells on which we aggregated the number/density of unique phone users associated to each phone antenna (NB: these maps were created with R standard packages for handling spatial data and



HUMAN MOBILITY

Mobile phones



From mobile phone data to the spatial structure of cities

Thomas Louail^{1,2}, Maxime Lenormand³, Oliva G. Cantu Ros⁴, Miguel Picornell⁴, Ricardo Herranz⁴, Enrique Frias-Martinez⁵, José J. Ramasco³ & Marc Barthelemy^{1,6}

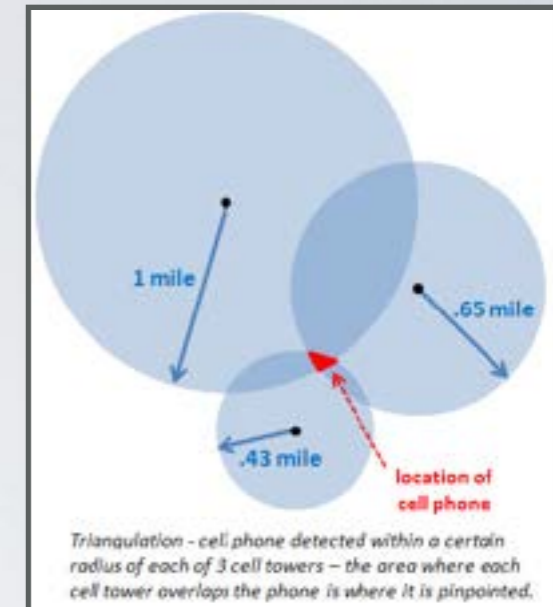


Figure 1 | The 31 Spanish urban areas with more than 200,000 inhabitants in 2011. Map of their locations and spatial extensions.

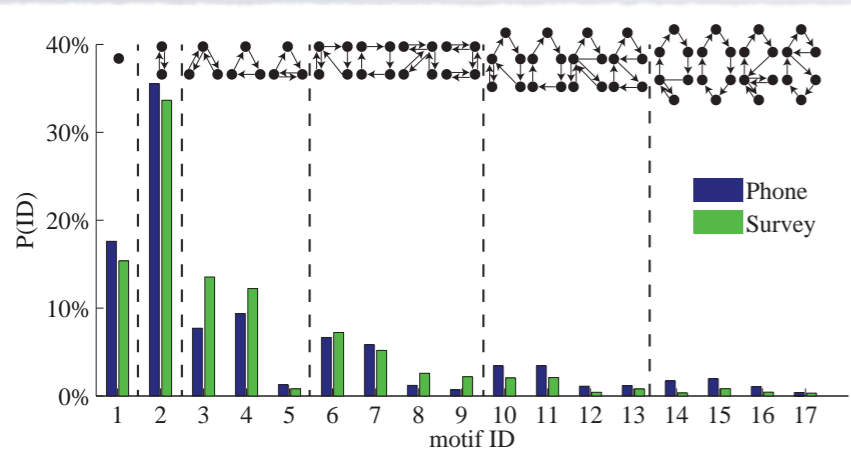


Figure 3.2: Frequent daily motifs. The 17 most frequent motifs account for over 90% of the measured daily trips. The distributions of the 17 motifs extracted from cell phone data and the Massachusetts travel survey are similar, and also conform to previous findings in Paris and

(Jiang, Fiore, Yang, Yingxiang, Ferreira, Frazzoli, González, 2013)

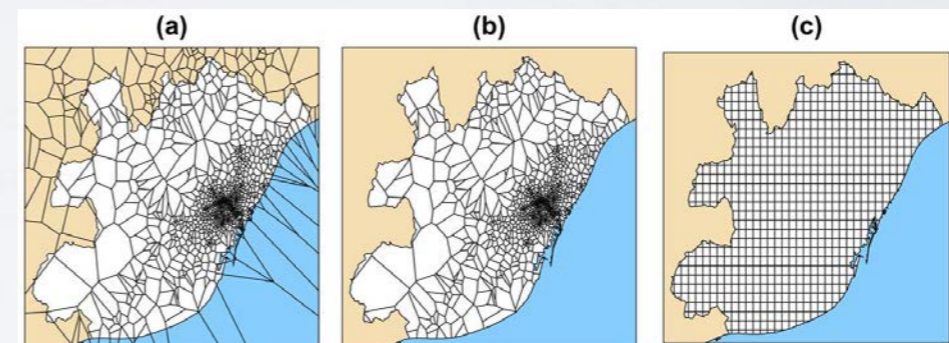
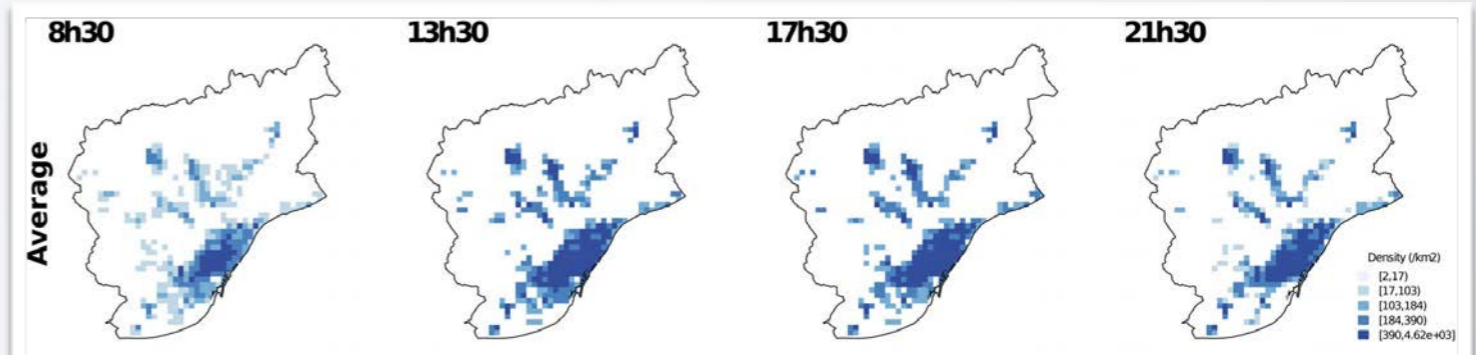


Figure 3 | Map of the metropolitan area of Barcelona. The white area represents the metropolitan area (administrative delimitation), the brown area represents territories surrounding the metropolitan area and the blue area the sea. (a) Voronoi cells of the mobile phone antennas point pattern. (b) Intersection between the Voronoi cells and the metropolitan area. (c) Grid composed of 1 km² square cells on which we aggregated the number/density of unique phone users associated to each phone antenna (NB: these maps were created with R standard packages for handling spatial data and



HUMAN MOBILITY CHECK-IN DATA

“**Friendship and Mobility: User Movement In Location-Based Social Networks**”,
Cho, Myers, Leskovec, *KDD'11*

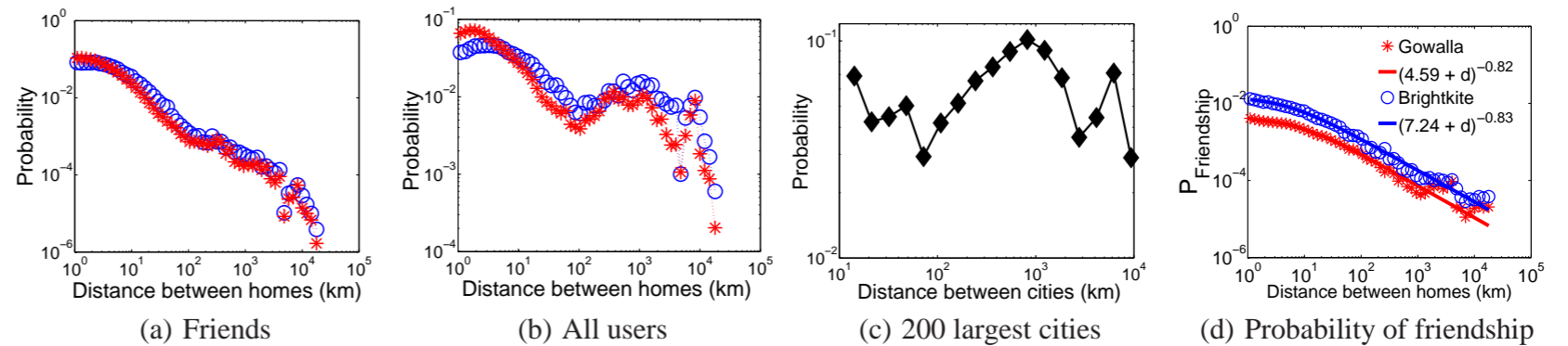
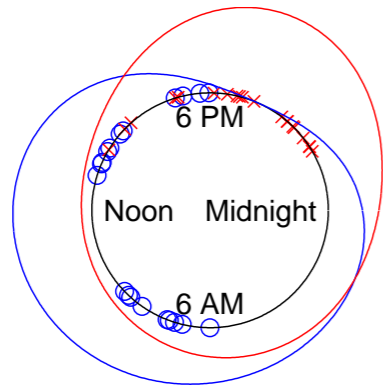


Figure 2: Distribution of home distances between (a) friends and (b) all users. (c) Distance between 200 world’s largest cities. (d) Probability of friendship as a function of distance when one accounts for non-uniform population density.



(a) Spatial model

(b) Temporal model

Figure 6: (a) Check-ins of a user in San Francisco: geographic distribution of check-ins when in home/work state. (b) Temporal model: distance to the red/blue line from the center is proportional the prob. of user being in home/work state.

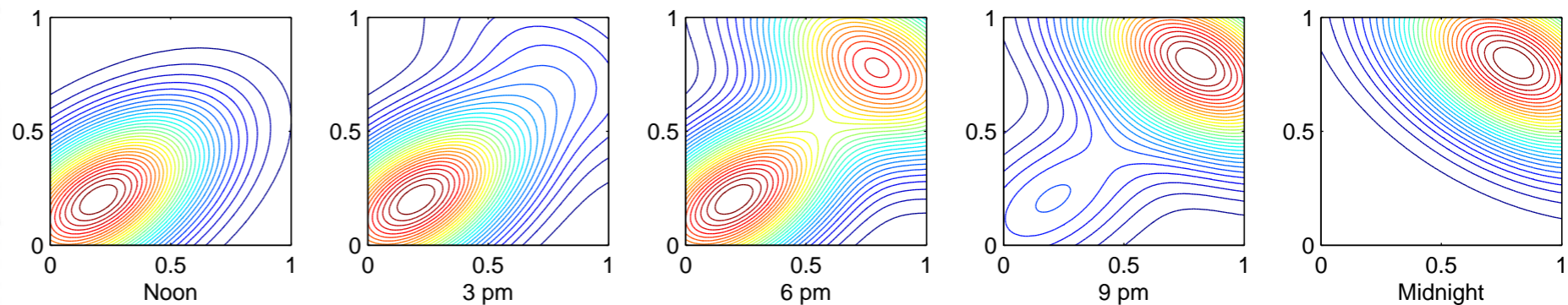
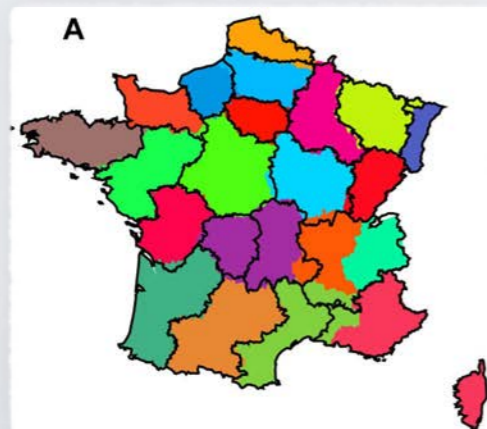
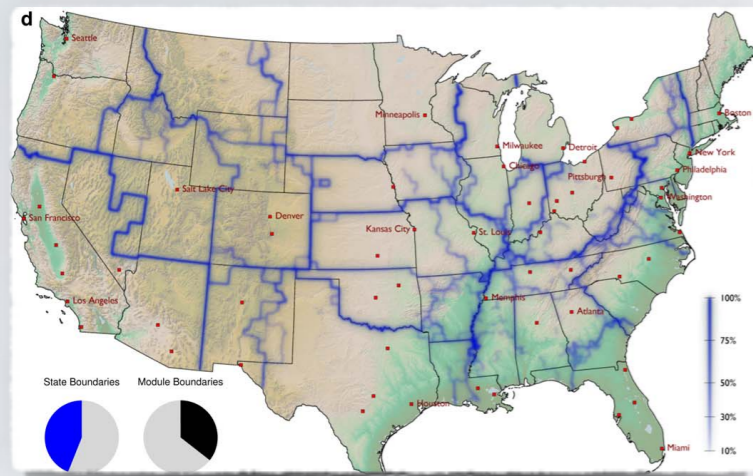


Figure 8: *Periodic Mobility Model*: Probability density of user location over time as user transitions from “work” to “home”.

GEOGRAPHIC 'COMMUNITIES'

Banknotes

- Thiemann, Theis, Grady, Brune, Brockmann, **"The Structure of Borders in a Small World"**, *PLoS One* 5(11):e15422, **2010**



Cell phone data

- Ratti, Sobolevsky, Calabrese, Andris, Reades, Martino, Claxton, Strogatz, **"Redrawing the Map of Great Britain from a Network of Human Interactions"**, *PLoS One*, 5(12):e14248, **2010**
- Calabrese, Dahlem, Gerber, Paul, Chen, Rowland, Rath, Ratti, **"The Connected States of America: Quantifying Social Radii of Influence"**, *IEEE 3rd Intl Conf on Social Computing (SocialCom)*, pp. 223-230, **2011**
- Sobolevsky, Szell, Campari, Couronné, Smoreda, Ratti, **"Delineating Geographical Regions with Networks of Human Interactions in an Extensive Set of Countries"**, *PLoS ONE* 8(12): e81707, **2013**

Check-in data

- Cranshaw, Schwartz, Hong, Sadeh, **"The Livehoods Project: Utilizing Social Media to Understand the Dynamics of a City"**, *ICWSM*, 58-65, **2012**
- Liu, Sui, Kang, Gao, **"Uncovering Patterns of Inter-Urban Trip and Spatial Interaction from Social Media Check-In Data"**, *PLoS One*,

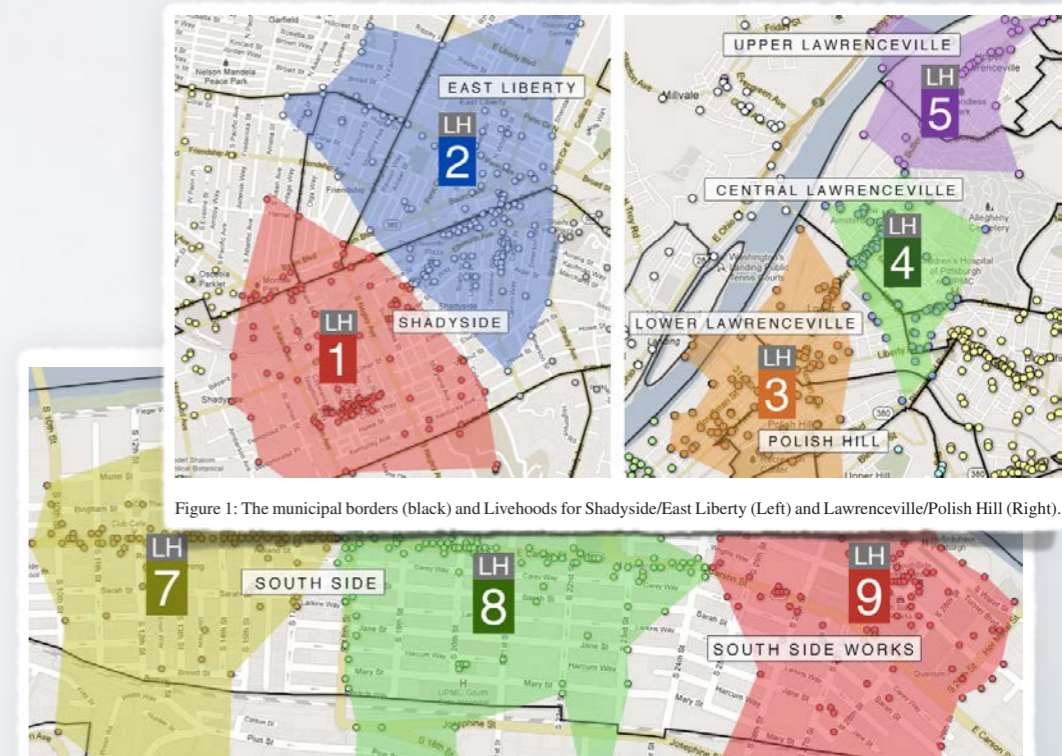
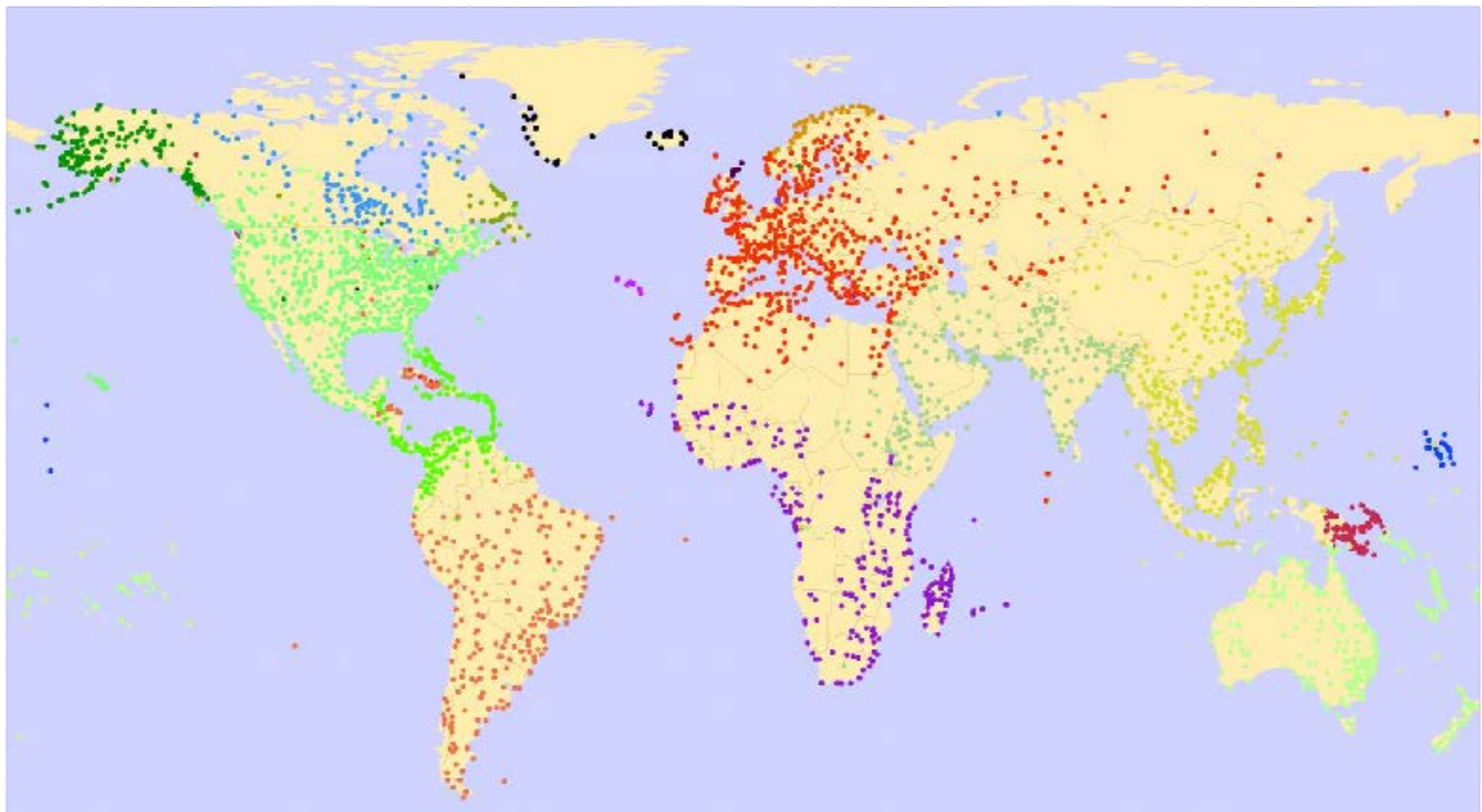


Figure 1: The municipal borders (black) and Livehoods for Shadyside/East Liberty (Left) and Lawrenceville/Polish Hill (Right).

Figure 2: The municipal borders (in black) and Livehoods for South Side.

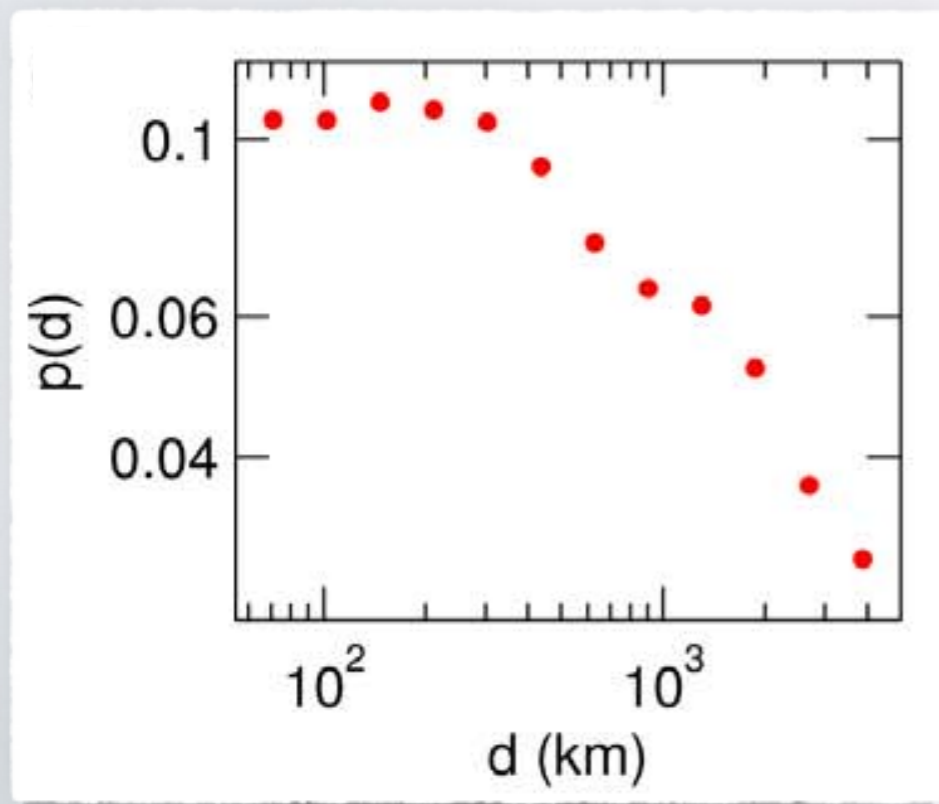
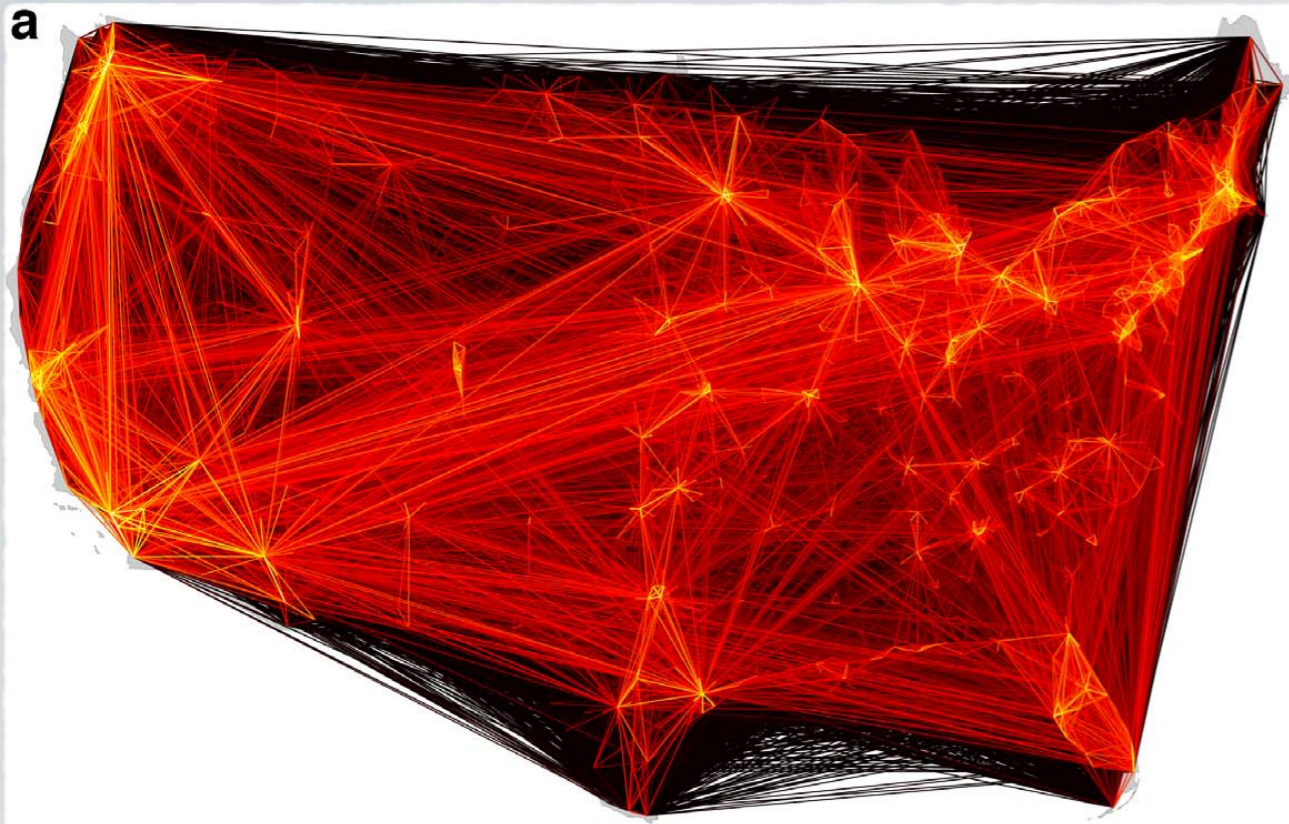
GEOGRAPHIC 'COMMUNITIES' SOME EARLY ATTEMPTS

Modularity-maximizing partition of communities in the
giant component of the worldwide airport network



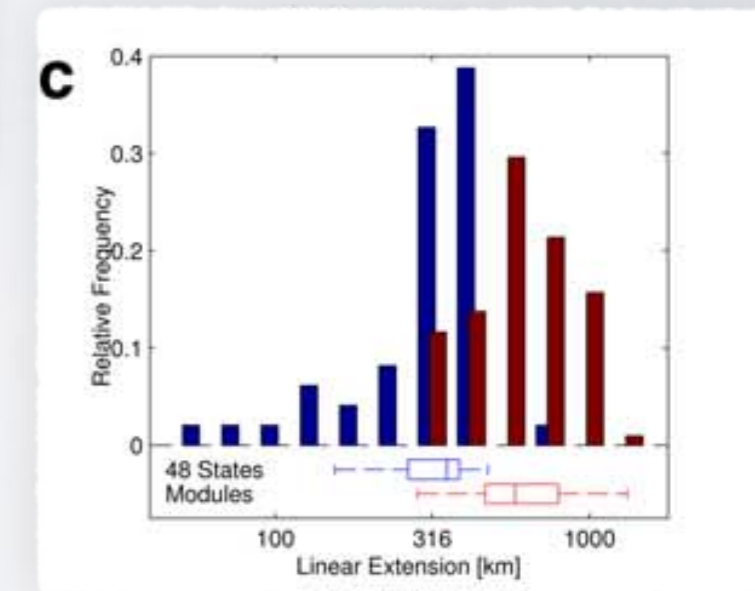
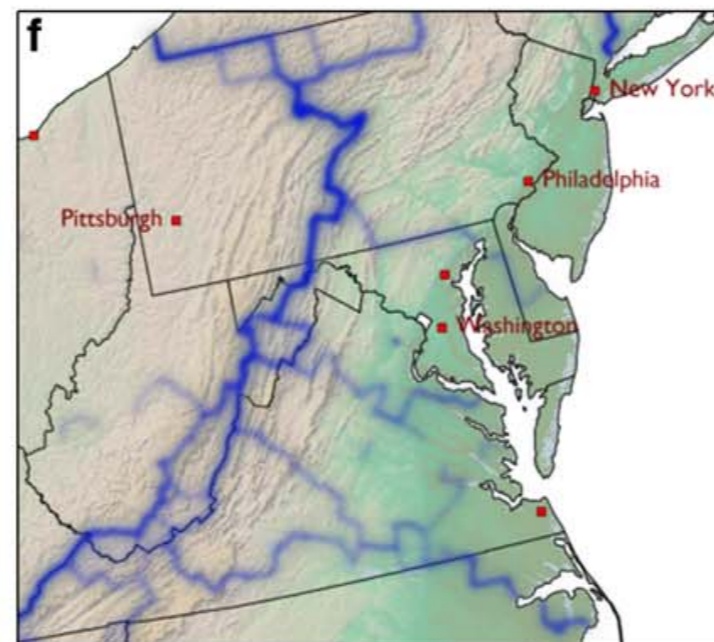
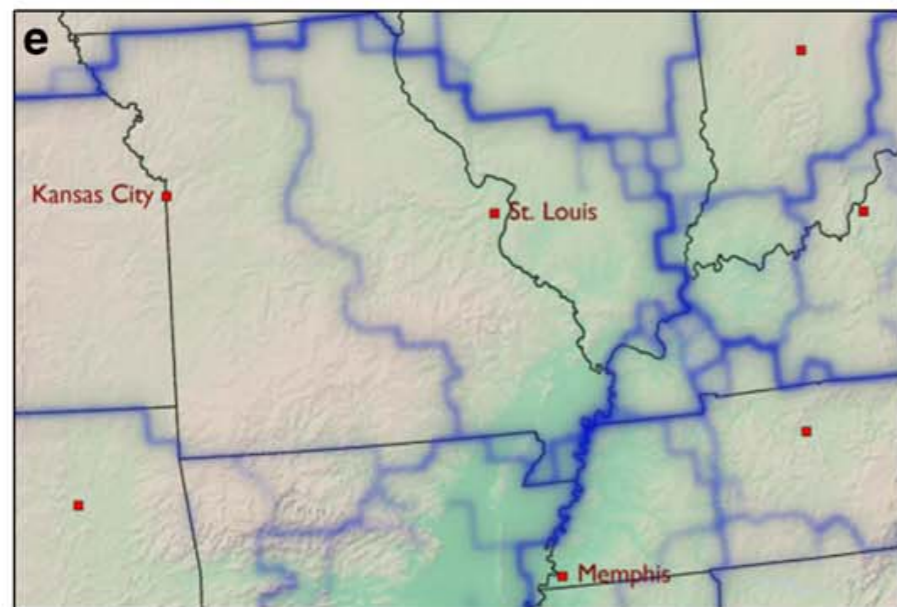
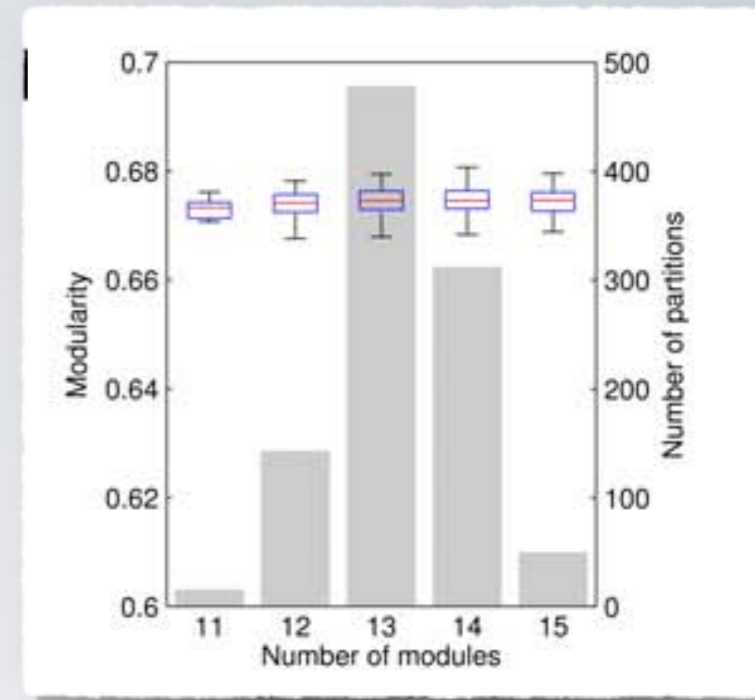
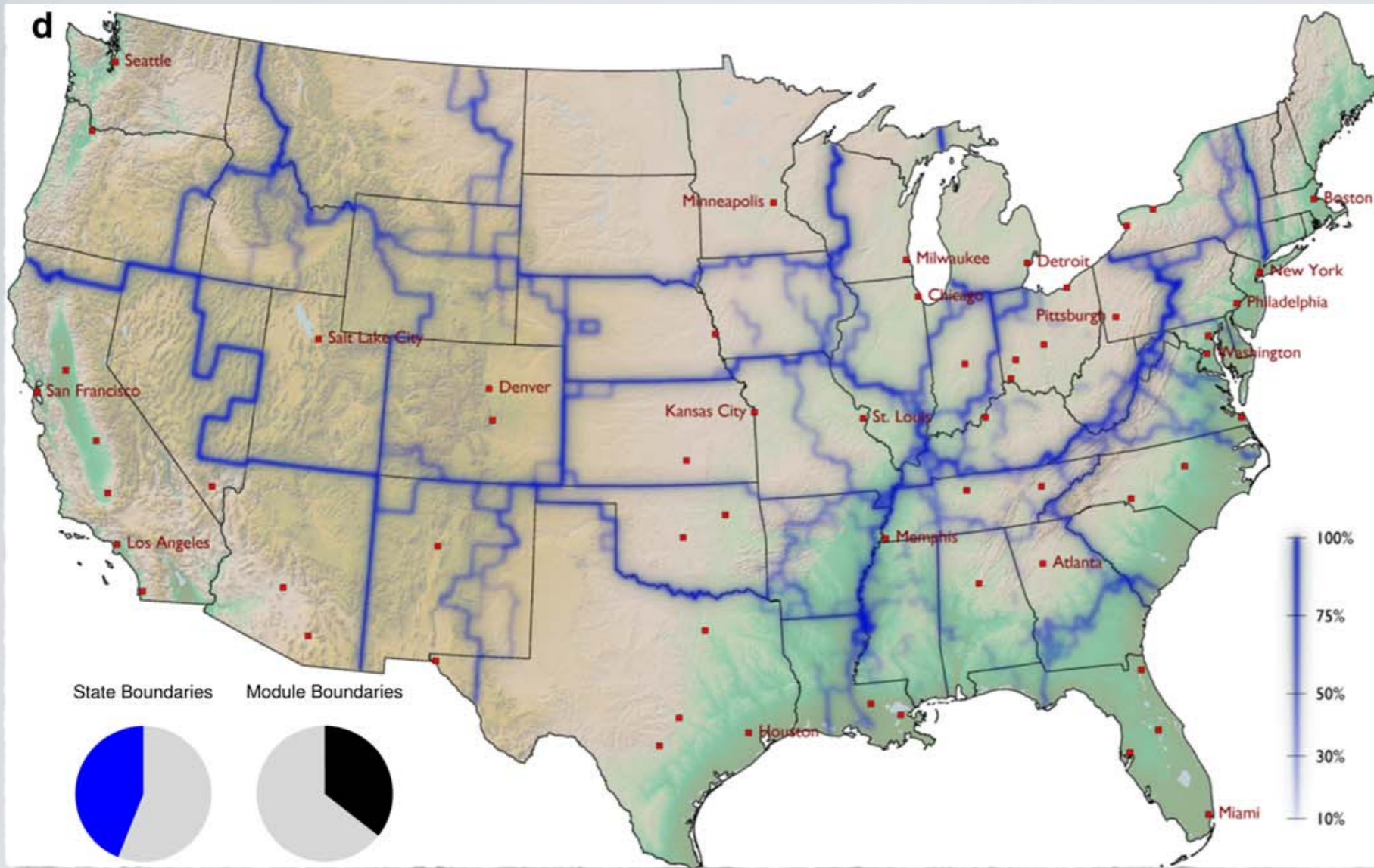
(Guimerà, Mossa, Turtschi, Amaral, 2005)

GEOGRAPHIC 'COMMUNITIES' BANK NOTES



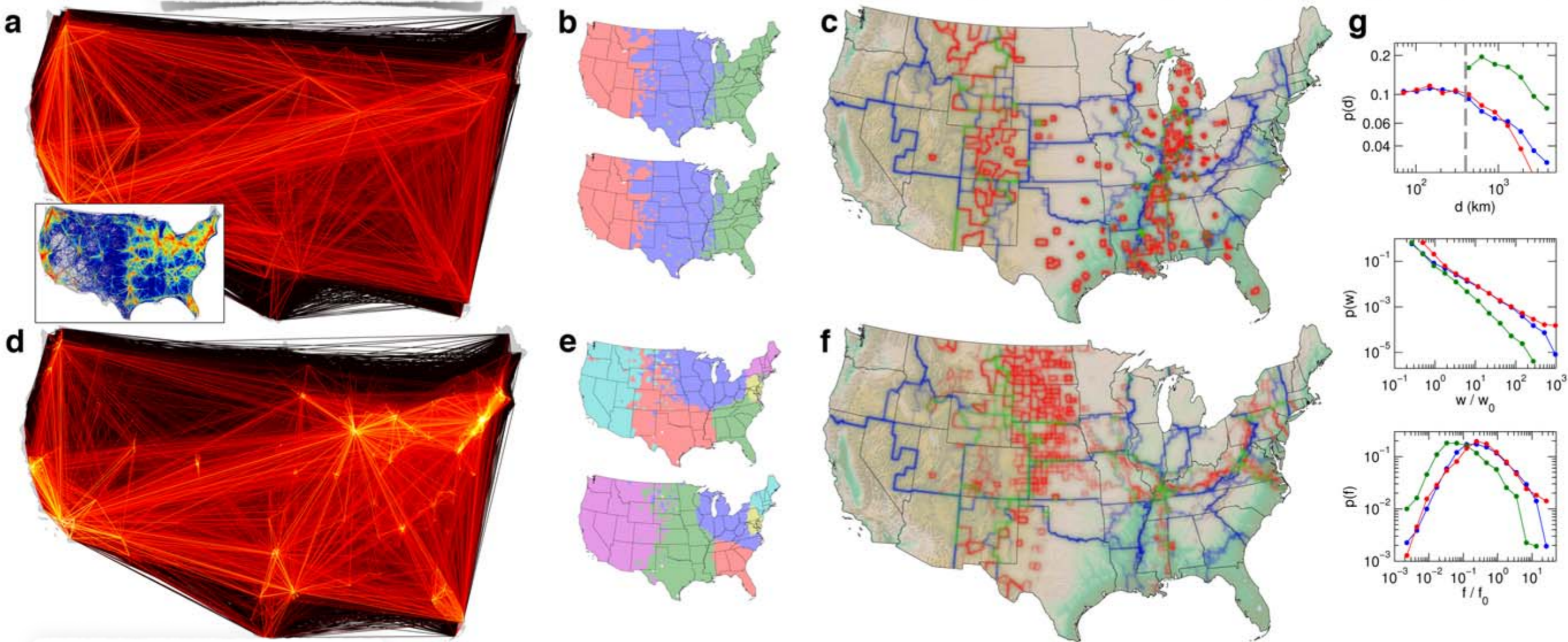
Thiemann, Theis, Grady,
Brune, Brockmann,
"The Structure of
Borders in a
Small World", *PLoS*
One 5(11):e15422,
2010

GEOGRAPHIC 'COMMUNITIES'



- Thiemann, Theis, Grady, Brune, Brockmann, "The Structure of Borders in a Small World", *PLoS One* 5(11):e15422, 2010

removing short distance links



reconstructing a gravity model

Figure 3. Comparative analysis of effective borders in two artificial systems: a modified mobility network deprived of short distance traffic (a–c), and a gravity model for human mobility (d–f). (a) A subnetwork of the original system (Fig. 1a) in which all links with geographic length $d < 400$ km are removed (the inset depicts the complementary, removed subnetwork). (b) Two generic partitions of this long-range network, consisting of only three modules that do not exhibit sharply defined geographical borders. (c) The resulting border structure (red lines) exhibits no significant overlap with the borders obtained from the original multi-scale system. Borders of the original system and overlap are depicted in blue and green, respectively. (d) A gravity model network as defined by Eq. (2). Parameters $\alpha = \beta = 0.96$ and $\mu = 0.3$ have been chosen to maximize first-order statistical similarity to the original data. (e) Although qualitatively the network in (d) shares features with the original network (Fig. 1a), generic partitions of the gravity model network are structurally different, typically exhibiting fewer modules per partition, in different locations and with less spatial compactness. (f) The border structure of the gravity network (red) partially coincides with the borders in the original data (blue), but not significantly. The overlap is shown in green, for significance tests see Text S1. (g) First order statistics of the two artificial networks in comparison to the original network. The functions $p(d)$, $p(w)$, and $p(f)$ for the long-range network in (a) (green), the gravity model network in (d) (red), and the

- Very different network than gravity models
- Without short- and medium-distance links, results are poor

• Thiemann, Theis, Grady, Brune, Brockmann, "The Structure of Borders in a Small World", *PLoS One* 5(11):e15422, 2010

GEOGRAPHIC 'COMMUNITIES' CELL PHONE DATA

- Ratti, Sobolevsky, Calabrese, Andris, Reades, Martino, Claxton, Strogatz, "**Redrawing the Map of Great Britain from a Network of Human Interactions**", *PLoS One*, 5(12):e14248, **2010**

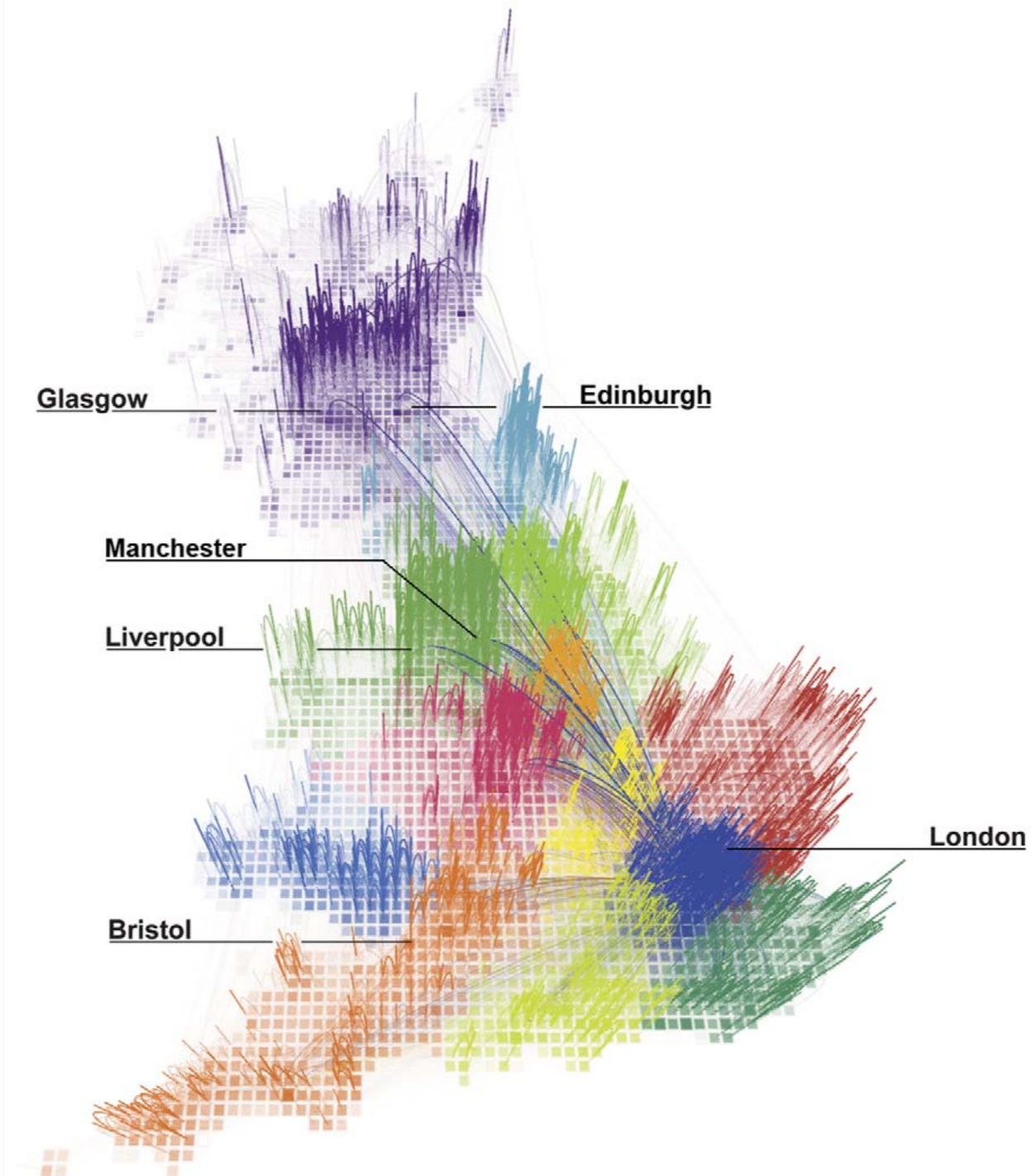


Figure 1. The geography of talk in Great Britain. This figure shows the strongest 80% of links, as measured by total talk time

GEOGRAPHIC 'COMMUNITIES' CELL PHONE DATA

- Ratti, Sobolevsky, Calabrese, Andris, Reades, Martino, Claxton, Strogatz, **"Redrawing the Map of Great Britain from a Network of Human Interactions"**, *PLoS One*, 5(12):e14248, **2010**

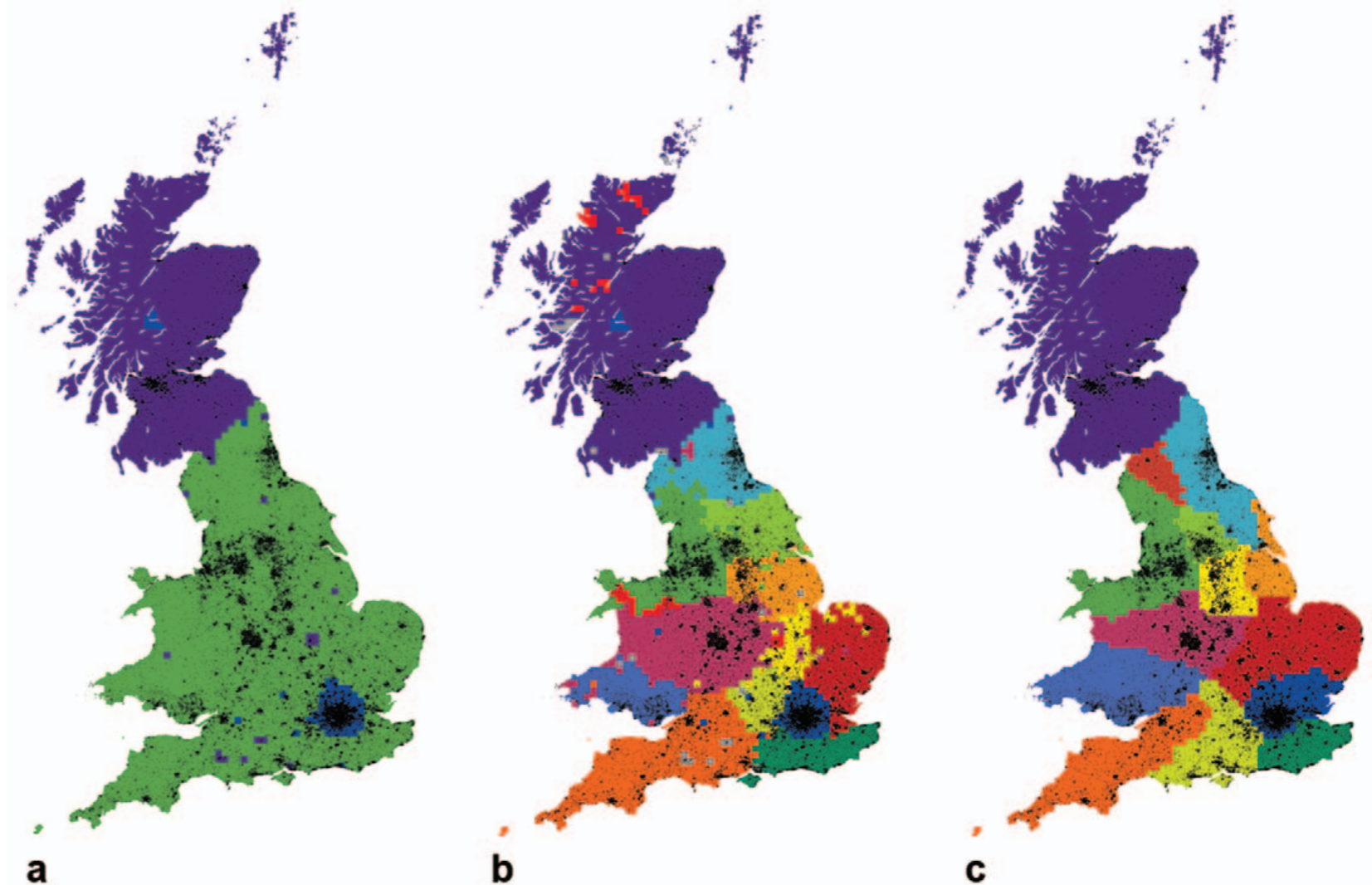
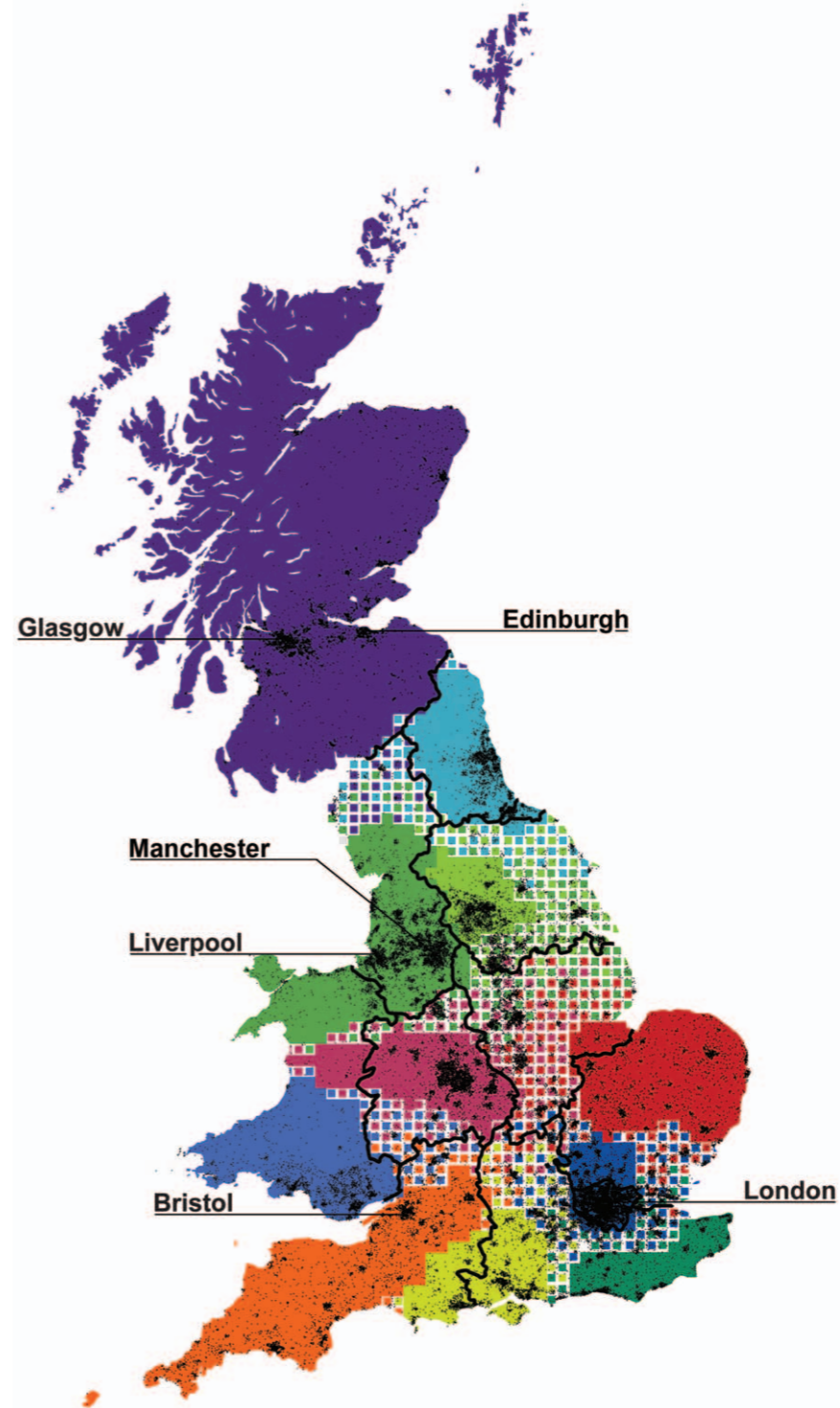


Figure 2. Defining regions through the spectral modularity optimization of telecommunications networks.

GEOGRAPHIC 'COMMUNITIES' CELL PHONE DATA

- Ratti, Sobolevsky, Calabrese, Andris, Reades, Martino, Claxton, Strogatz, **"Redrawing the Map of Great Britain from a Network of Human Interactions"**, *PLoS One*, 5(12):e14248, **2010**



GEOGRAPHIC 'COMMUNITIES' CELL PHONE DATA

- Ratti, Sobolevsky, Calabrese, Andris, Reades, Martino, Claxton, Strogatz, **"Redrawing the Map of Great Britain from a Network of Human Interactions"**, *PLoS One*, 5(12):e14248, **2010**
- Calabrese, Dahlem, Gerber, Paul, Chen, Rowland, Rath, Ratti, **"The Connected States of America: Quantifying Social Radii of Influence"**, *IEEE 3rd Intl Conf on Social Computing (SocialCom)*, pp. 223-230, **2011**

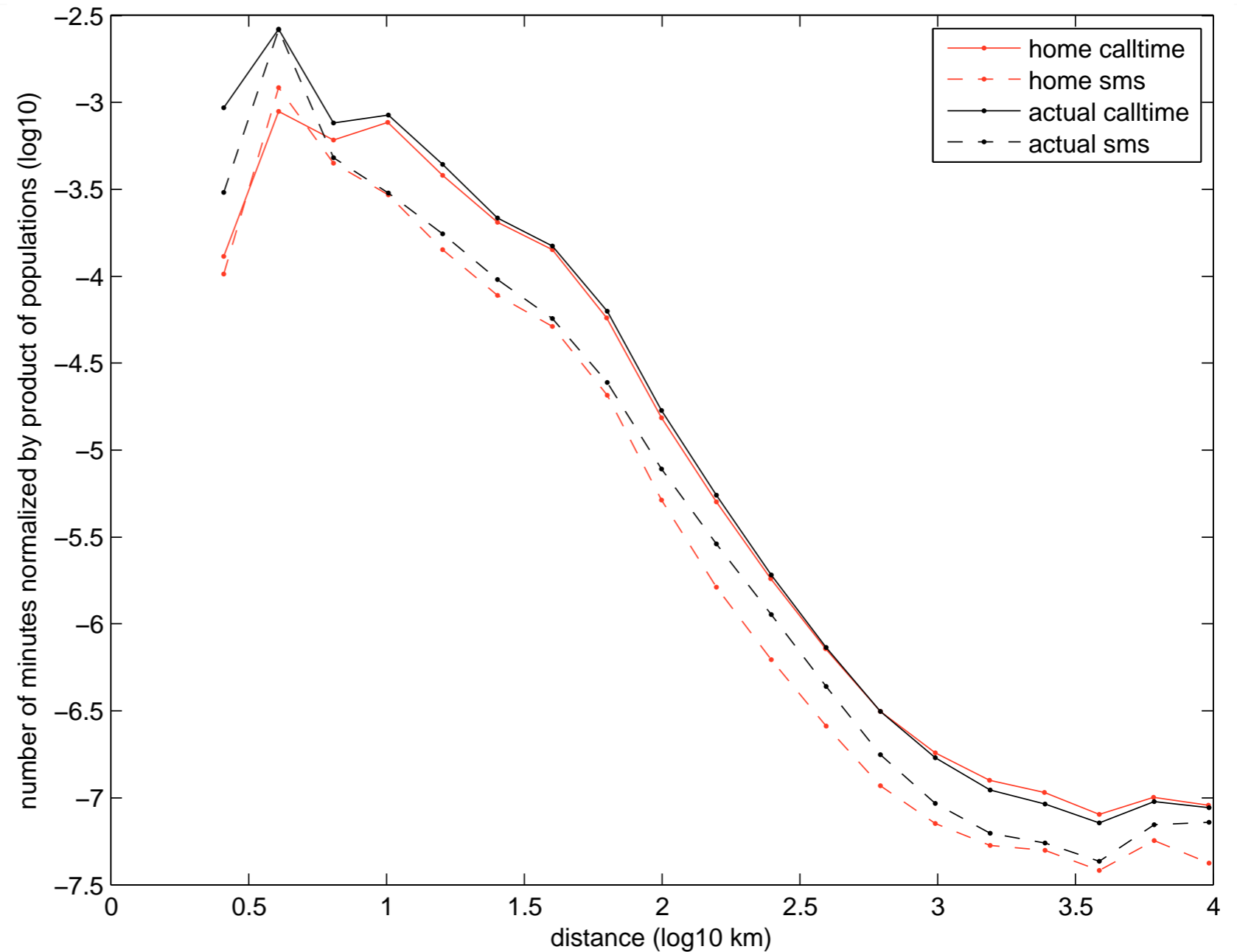


Fig. 2. Distance decay comparison - Communication networks

GEOGRAPHIC 'COMMUNITIES'

CELL PHONE DATA

- Ratti, Sobolevsky, Calabrese, Andris, Reades, Martino, Claxton, Strogatz, "**Redrawing the Map of Great Britain from a Network of Human Interactions**", *PLoS One*, 5(12):e14248, **2010**
- Calabrese, Dahlem, Gerber, Paul, Chen, Rowland, Rath, Ratti, "**The Connected States of America: Quantifying Social Radii of Influence**", *IEEE 3rd Intl Conf on Social Computing (SocialCom)*, pp. 223-230, **2011**

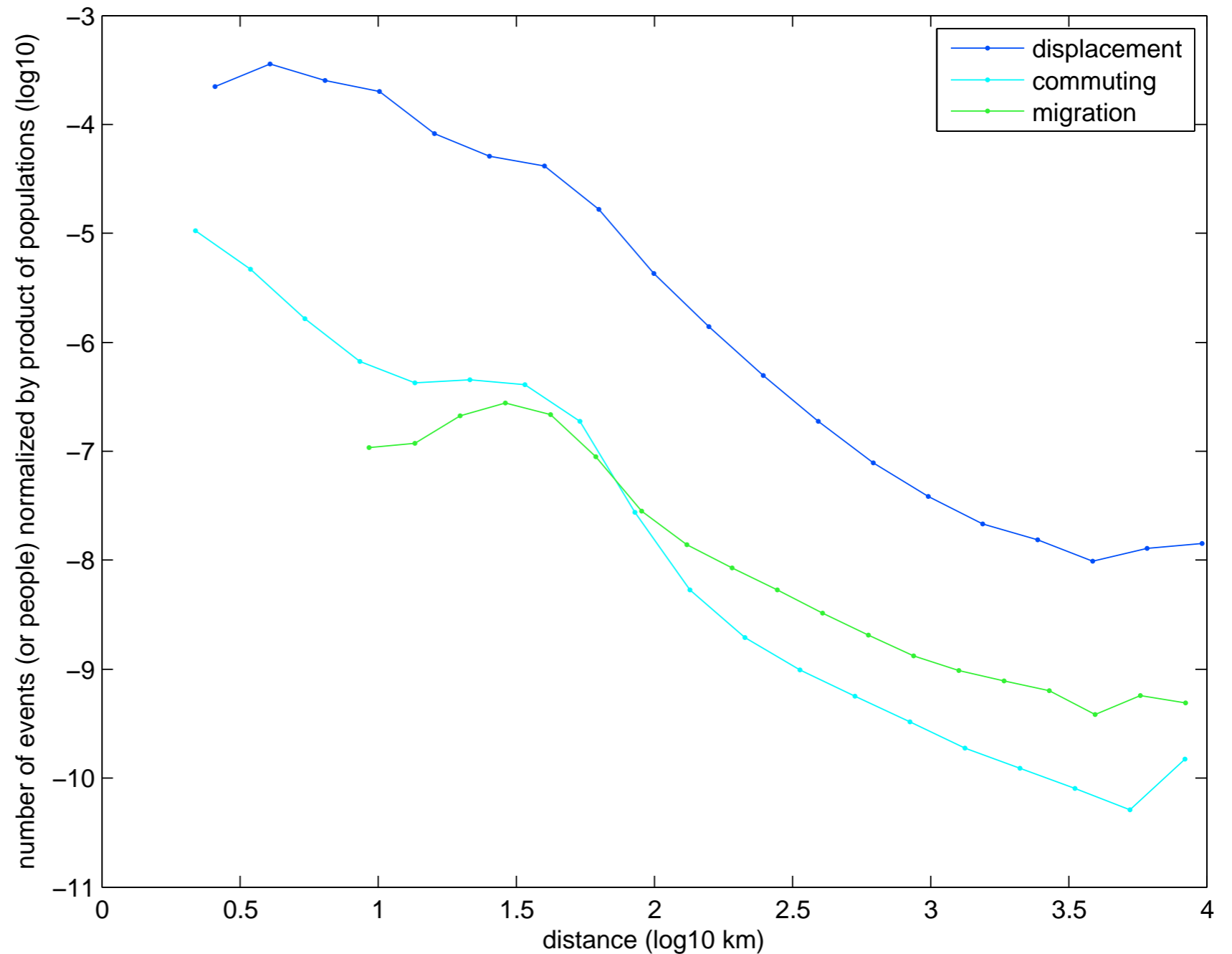


Fig. 3. Distance decay comparison - Mobility networks

GEOGRAPHIC 'COMMUNITIES' CELL PHONE DATA

- Ratti, Sobolevsky, Calabrese, Andris, Reades, Martino, Claxton, Strogatz, **"Redrawing the Map of Great Britain from a Network of Human Interactions"**, *PLoS One*, 5(12):e14248, **2010**
- Calabrese, Dahlem, Gerber, Paul, Chen, Rowland, Rath, Ratti, **"The Connected States of America: Quantifying Social Radii of Influence"**, *IEEE 3rd Intl Conf on Social Computing (SocialCom)*, pp. 223-230, **2011**

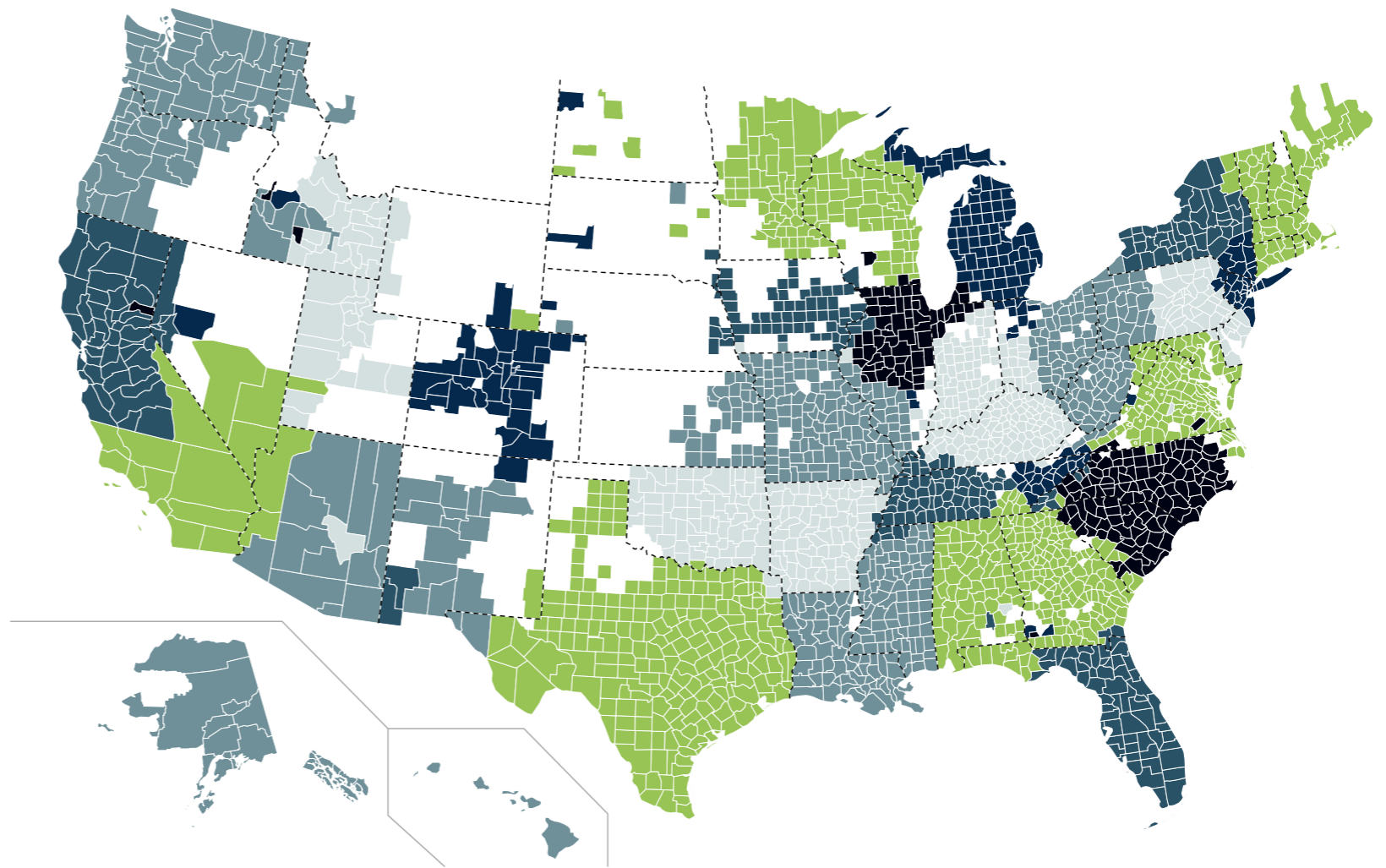
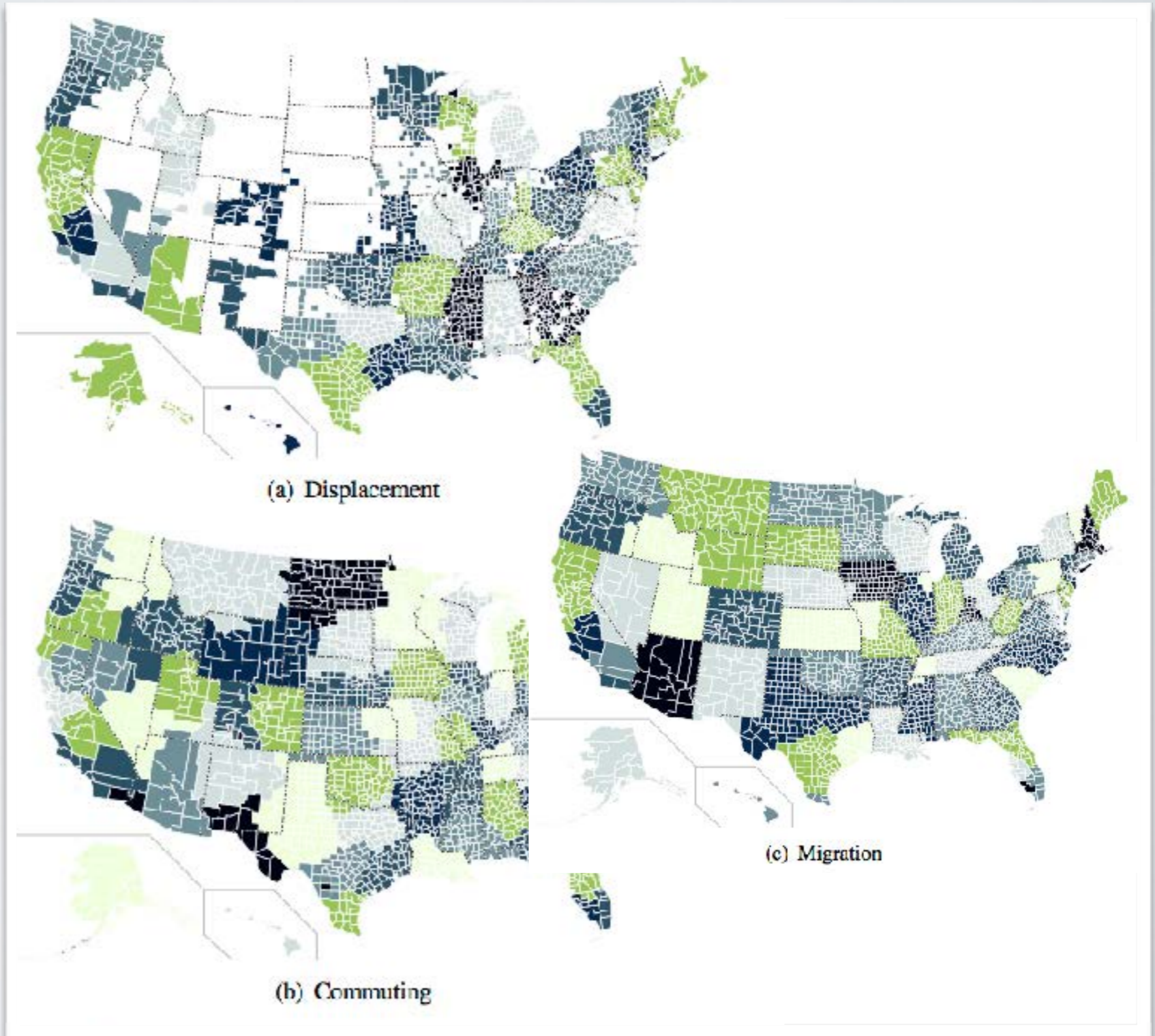


Fig. 4. Communities structure in the home location network with call-time weights. Puerto Rico has its own community (not shown).

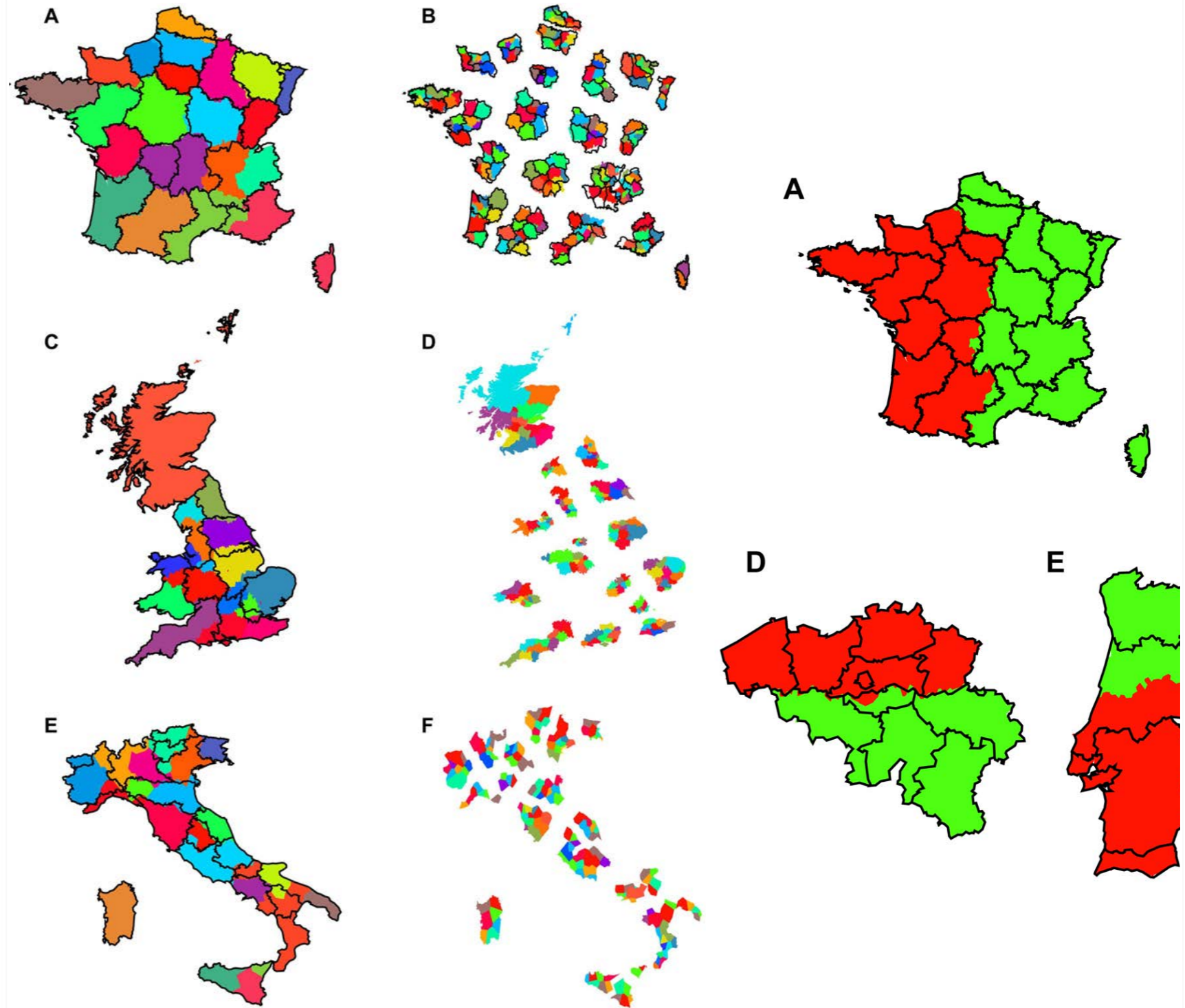
GEOGRAPHIC 'COMMUNITIES' CELL PHONE DATA

- Ratti, Sobolevsky, Calabrese, Andris, Reades, Martino, Claxton, Strogatz, "**Redrawing the Map of Great Britain from a Network of Human Interactions**", *PLoS One*, 5(12):e14248, **2010**
- Calabrese, Dahlem, Gerber, Paul, Chen, Rowland, Rath, Ratti, "**The Connected States of America: Quantifying Social Radii of Influence**", *IEEE 3rd Intl Conf on Social Computing (SocialCom)*, pp. 223-230, **2011**



GEOGRAPHIC 'COMMUNITIES' CELL PHONE DATA

- Ratti, Sobolevsky, Calabrese, Andris, Reades, Martino, Claxton, Strogatz, **"Redrawing the Map of Great Britain from a Network of Human Interactions"**, *PLoS One*, 5(12):e14248, **2010**
- Calabrese, Dahlem, Gerber, Paul, Chen, Rowland, Rath, Ratti, **"The Connected States of America: Quantifying Social Radii of Influence"**, *IEEE 3rd Intl Conf on Social Computing (SocialCom)*, pp. 223-230, **2011**
- Sobolevsky, Szell, Campari, Couronné, Smoreda, Ratti, **"Delineating Geographical Regions with Networks of Human Interactions in an Extensive Set of Countries"**, *PLoS ONE* 8(12): e81707, **2013**



GEOGRAPHIC 'COMMUNITIES' CHECK-IN DATA

- Cranshaw, Schwartz, Hong, Sadeh, "**The Livehoods Project: Utilizing Social Media to Understand the Dynamics of a City**", *ICWSM*, 58-65, 2012

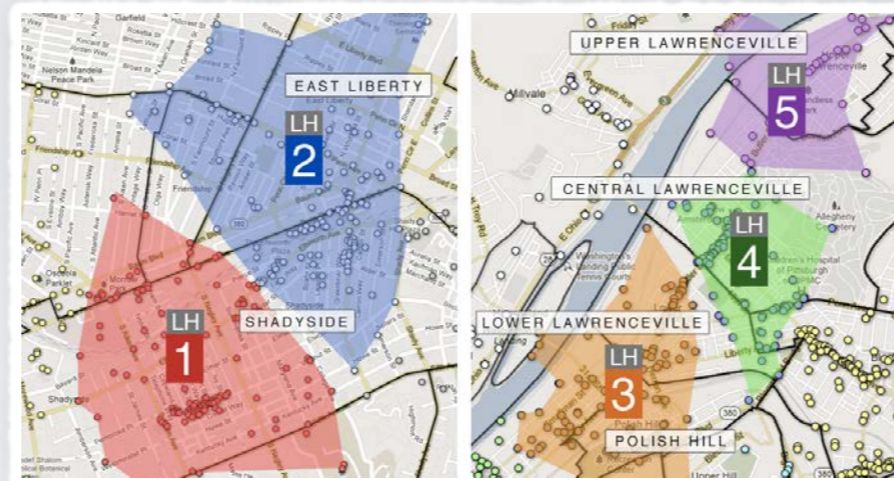


Figure 1: The municipal borders (black) and Livehoods for Shadyside/East Liberty (Left) and Lawrenceville/Polish Hill (Right).

Shadyside and East Liberty: In the fall of 2002, a Whole Foods Market opened in Pittsburgh directly on the border of two very distinct neighborhoods – East Liberty to the north and Shadyside to the south, separated by train tracks and a public busway. East Liberty, once the third-largest retail center in Pennsylvania, has suffered the pains of decades of neglect which led to high crime rates and a demographic population consisting of mainly low income, predominantly black residents. On literally the other side of the tracks is Shadyside, one of the most coveted neighborhoods, characterized in our interviews as a wealthy, predominately white neighborhood (O’Toole 2010). The upscale grocery store that was situated between them was the first component of “East Side,” a multi-phase development project in East Liberty orchestrated by The Mosites Company, a local real-estate firm. Since the opening of Whole Foods, the surrounding area has been massively transformed, consequently affecting patterns of behavior for both local residents and visitors.

That makes sense to me because I think at one point it was more walled off and this was poor [East Liberty] and this was wealthy [Shadyside] and now there are nice places in East Liberty and there’s some more diversity in this area so they are becoming more the same. And I do think Shadyside is almost shrinking and you only do have a few streets that are really that wealthy and bougie any more.

- Use check-in data from Foursquare in Pittsburgh to create a matrix users x locations
... then (cosine) similarities between places...
... and then clusters (k eigenvectors).
- Compare the results with interviews with 27 inhabitants – quali-quantitative study

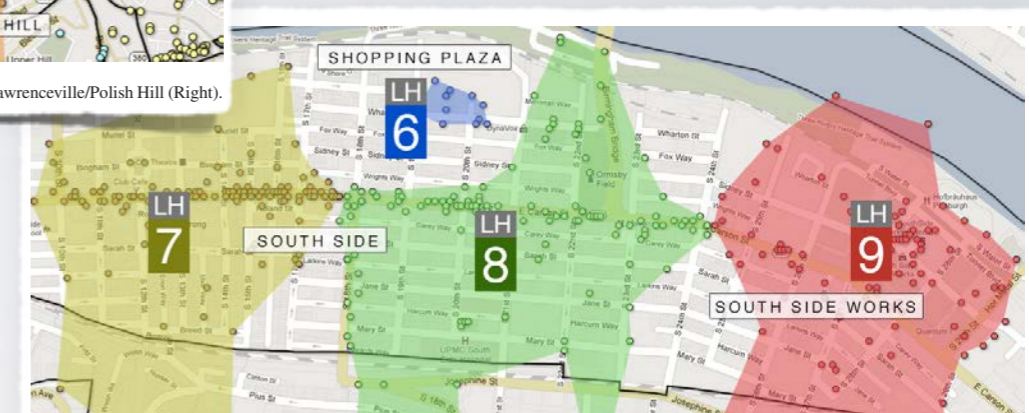


Figure 2: The municipal borders (in black) and Livehoods for South Side.

Demographics: In our interviews, we found strong evidence that the demographics of the residents and visitors of an area often played a strong role in explaining the divisions between Livehoods. As mentioned above, South Side was *split* by the algorithm into 4 different Livehoods. Our interviewees characterized each of these differently based on the type of people who visit them. For example, LH9 was described as a newly developed area harboring national chain stores in contrast to the more local, mostly night-life oriented area of LH7—each attracting different demographics.

GEOGRAPHIC 'COMMUNITIES' CHECK-IN DATA

- Cranshaw, Schwartz, Hong, Sadeh, "**The Livelihoods Project: Utilizing Social Media to Understand the Dynamics of a City**", *ICWSM*, 58-65, 2012
- Liu, Sui, Kang, Gao, "**Uncovering Patterns of Inter-Urban Trip and Spatial Interaction from Social Media Check-In**"

- temporally and geographically tagged "check-ins", from which it is possible to derive trajectories (from A to B and then B to C, etc.).
- yields a weighted network, onto which community detection is eventually applied
- Two methodological insights:
 - using Voronoi polygons to group check-ins into "cities" (but apparently starts from a predefined list of cities, which are the centers of the Voronoi paving).
 - fitting pretty well a gravity model for check-ins and flights, exhibiting distinct exponents for short- and long-distance

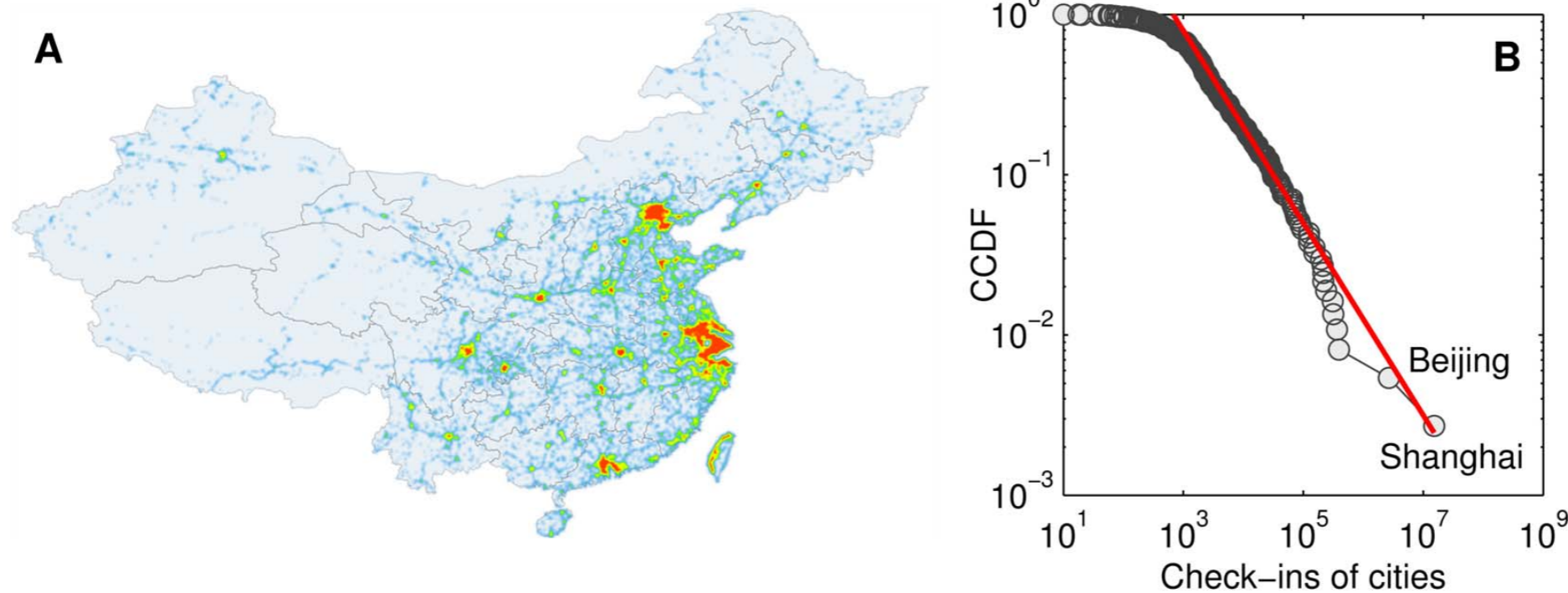


Figure 1. Heat map of all check-in points and frequency distribution of check-ins in the 370 cities. (A) The map, created using density estimation, clearly depicts the distributions of cities and transportation networks in China. Note that The South China Sea Islands are not shown for simplicity. (B) As shown by the CCDF (complementary cumulative distribution function), the frequency distribution exhibits a heavy tail characteristic. Shanghai and Beijing, the two biggest cities in China, have the most check-in records.

GEOGRAPHIC 'COMMUNITIES' CHECK-IN DATA

- Cranshaw, Schwartz, Hong, Sadeh, "**The Livelihoods Project: Utilizing Social Media to Understand the Dynamics of a City**", *ICWSM*, 58-65, 2012
- Liu, Sui, Kang, Gao, "**Uncovering Patterns of Inter-Urban Trip and Spatial Interaction from Social Media Check-In**

- temporally and geographically tagged "check-ins", from which it is possible to derive trajectories (from A to B and then B to C, etc.).
- yields a weighted network, onto which community detection is eventually applied
- Two methodological insights:
 - using Voronoi polygons to group check-ins into "cities" (but apparently starts from a predefined list of cities, which are the centers of the Voronoi paving).
 - fitting pretty well a gravity model for check-ins and flights, exhibiting distinct exponents for short- and long-distance

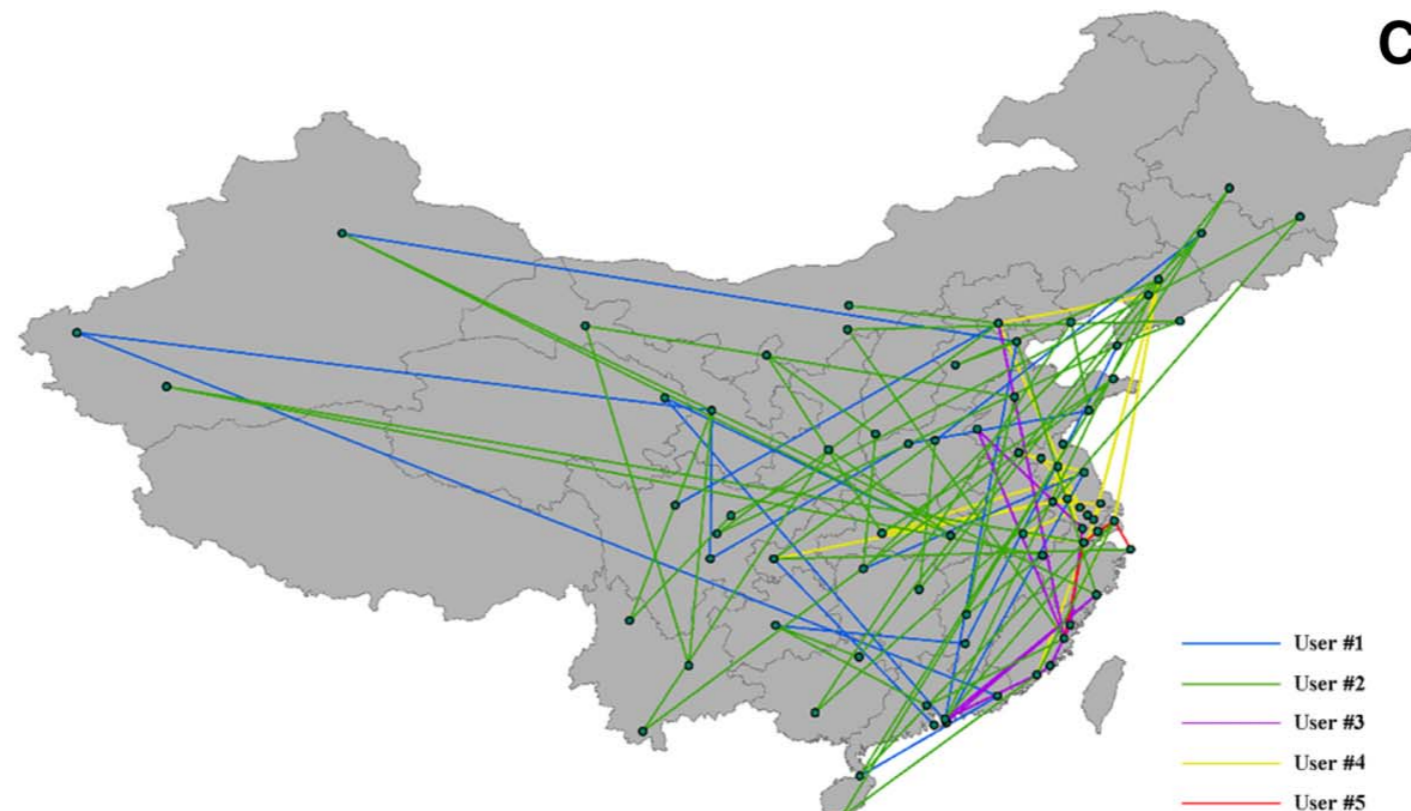


Figure 2. Characteristics of check-ins from the perspective of users. For each user, w

GEOGRAPHIC 'COMMUNITIES' CHECK-IN DATA

- Cranshaw, Schwartz, Hong, Sadeh, "**The Livelihoods Project: Utilizing Social Media to Understand the Dynamics of a City**", *ICWSM*, 58-65, 2012
- Liu, Sui, Kang, Gao, "**Uncovering Patterns of Inter-Urban Trip and Spatial Interaction from Social Media Check-In**"

- temporally and geographically tagged "check-ins", from which it is possible to derive trajectories (from A to B and then B to C, etc.).
- yields a weighted network, onto which community detection is eventually applied
- Two methodological insights:
 - using Voronoi polygons to group check-ins into "cities" (but apparently starts from a predefined list of cities, which are the centers of the Voronoi paving).
 - fitting pretty well a gravity model for check-ins and flights, exhibiting distinct exponents for short- and long-distance

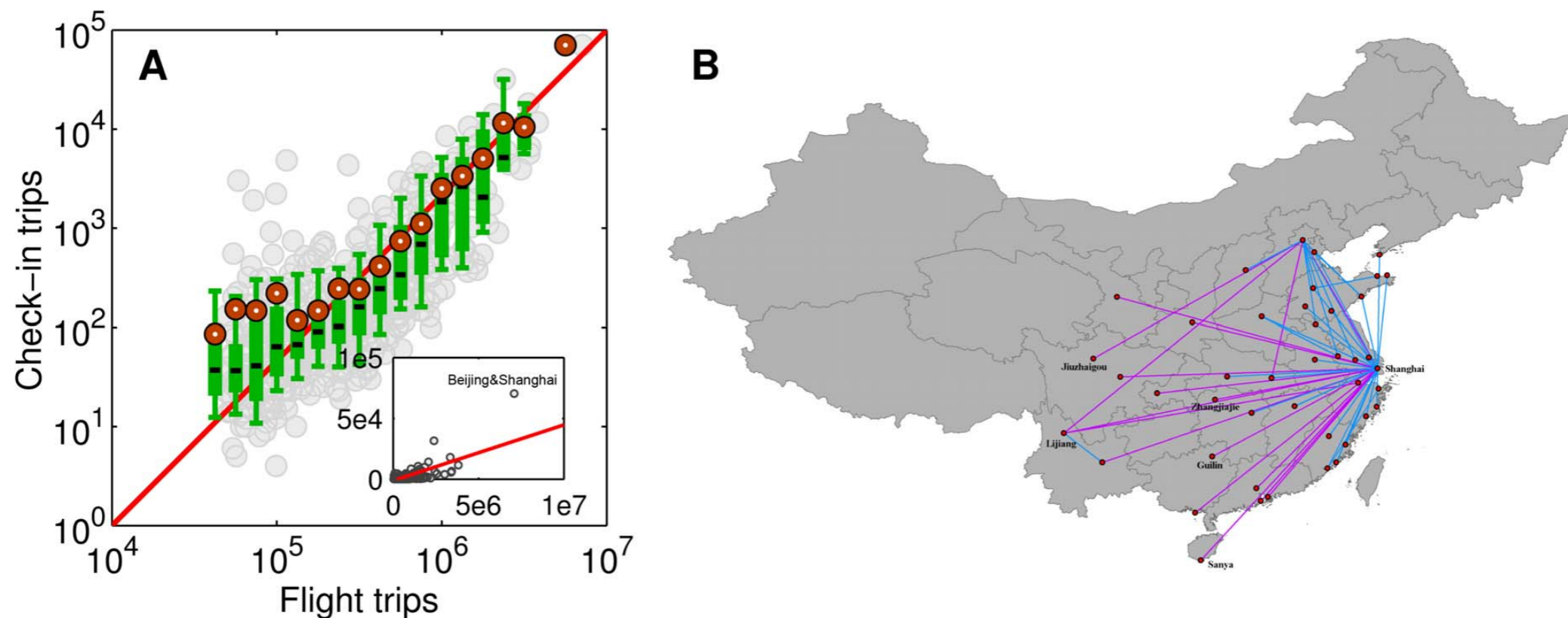


Figure 3. Comparison between trips extracted from check-in records, denoted by T_{cij} , and flight trips T_{fij} . (A) Scatter plot of T_{cij} versus T_{fij} , indicating a weak positive correlation. (B) 50 city pairs with the top highest T_{cij}/T_{fij} .

GEOGRAPHIC 'COMMUNITIES' CHECK-IN DATA

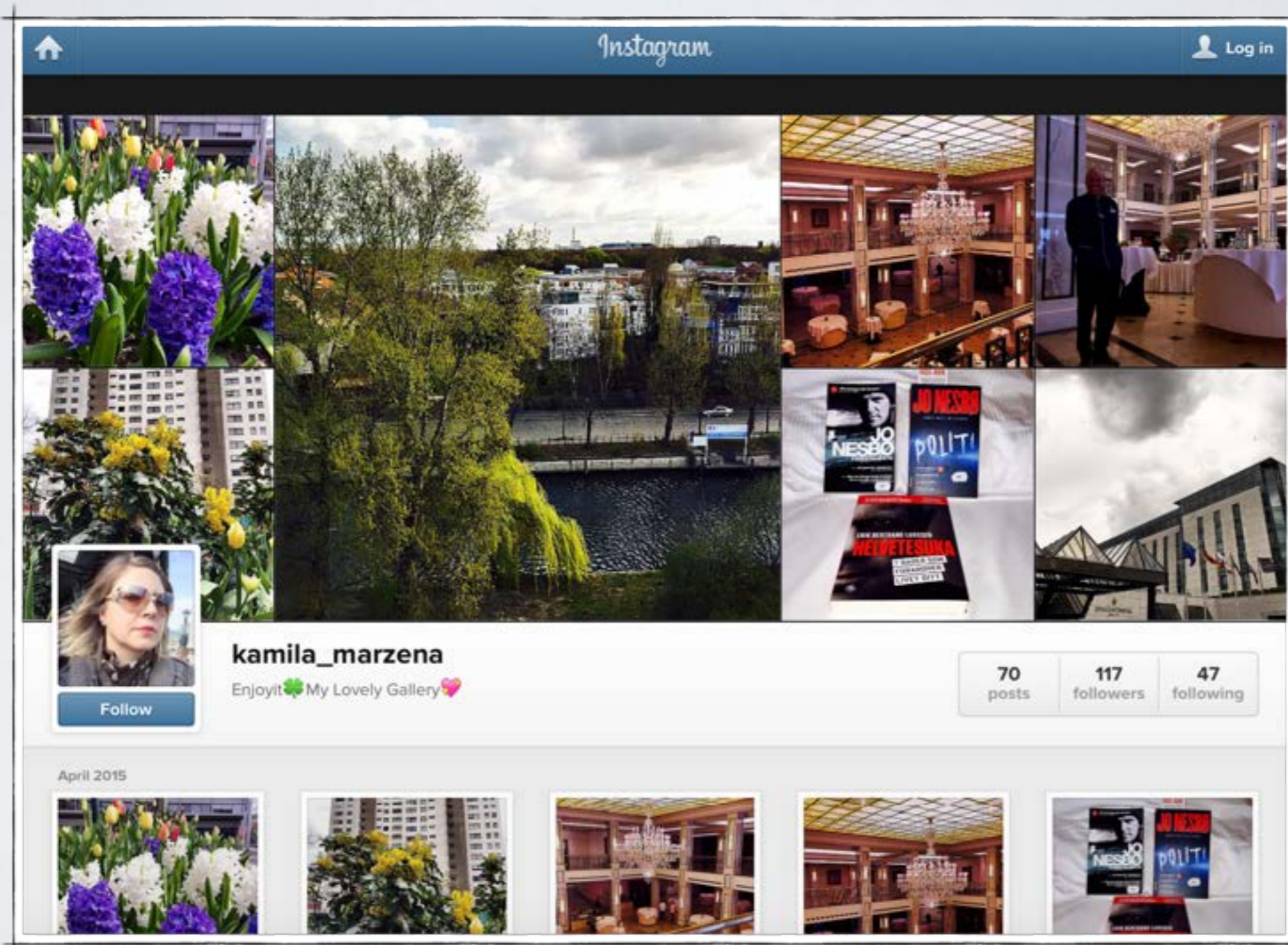
- Cranshaw, Schwartz, Hong, Sadeh, "**The Livelihoods Project: Utilizing Social Media to Understand the Dynamics of a City**", *ICWSM*, 58-65, 2012
- Liu, Sui, Kang, Gao, "**Uncovering Patterns of Inter-Urban Trip and Spatial Interaction from Social Media Check-In**

- temporally and geographically tagged "check-ins", from which it is possible to derive trajectories (from A to B and then B to C, etc.).
- yields a weighted network, onto which community detection is eventually applied
- Two methodological insights:
 - using Voronoi polygons to group check-ins into "cities" (but apparently starts from a predefined list of cities, which are the centers of the Voronoi paving).
 - fitting pretty well a gravity model for check-ins and flights, exhibiting distinct exponents for short- and long-distance



Figure 9. Communities detected from the interaction network G . We run the multilevel algorithm 20 times, each of which yields a partition. By merging the Voronoi polygons of cities in the same community, a partition can be visualized. Regions with thicker borders indicate that they occur in more partitions.

GHOST BORDERS OF INSTAGRAM

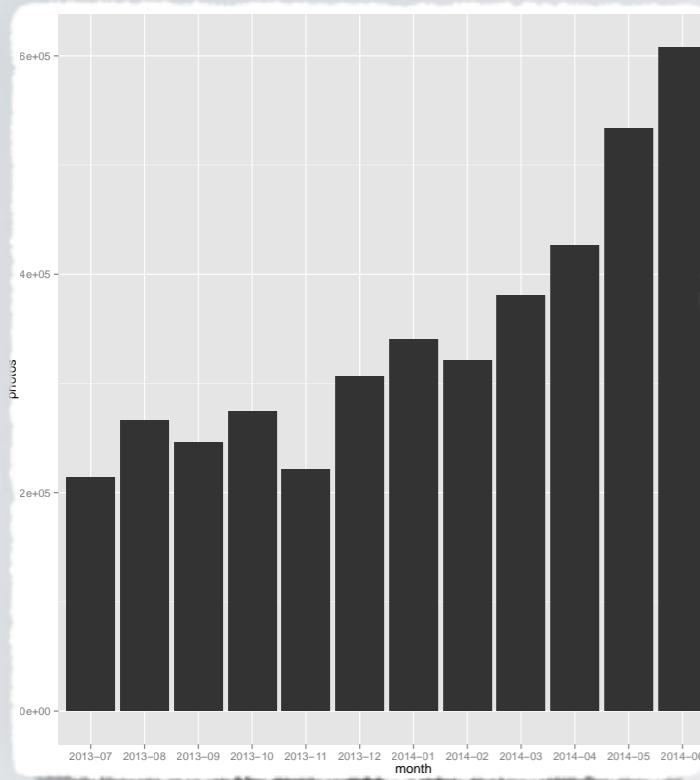


- Menezes, Roth; 2017

DATA COLLECTION

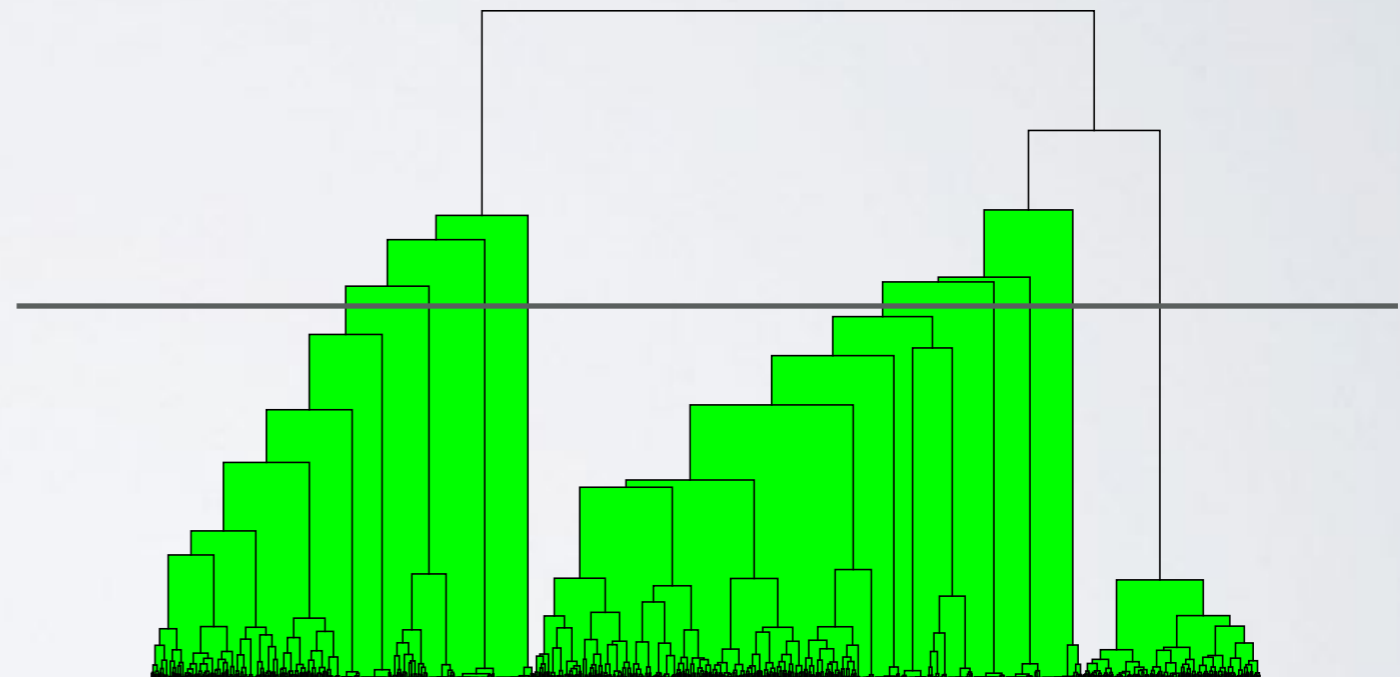
- Instagram API
- Request all photos from a 5 Km radius around a specified point, within a time window
- Make requests for coordinates of all locations with population > 500
- Discard duplicates (from radius overlaps)
- Data - set of meta-data for pictures
 - Author's user id
 - Timestamp
 - Coordinates
 - Comments (also with user id and timestamp)

USAGE FEATURES

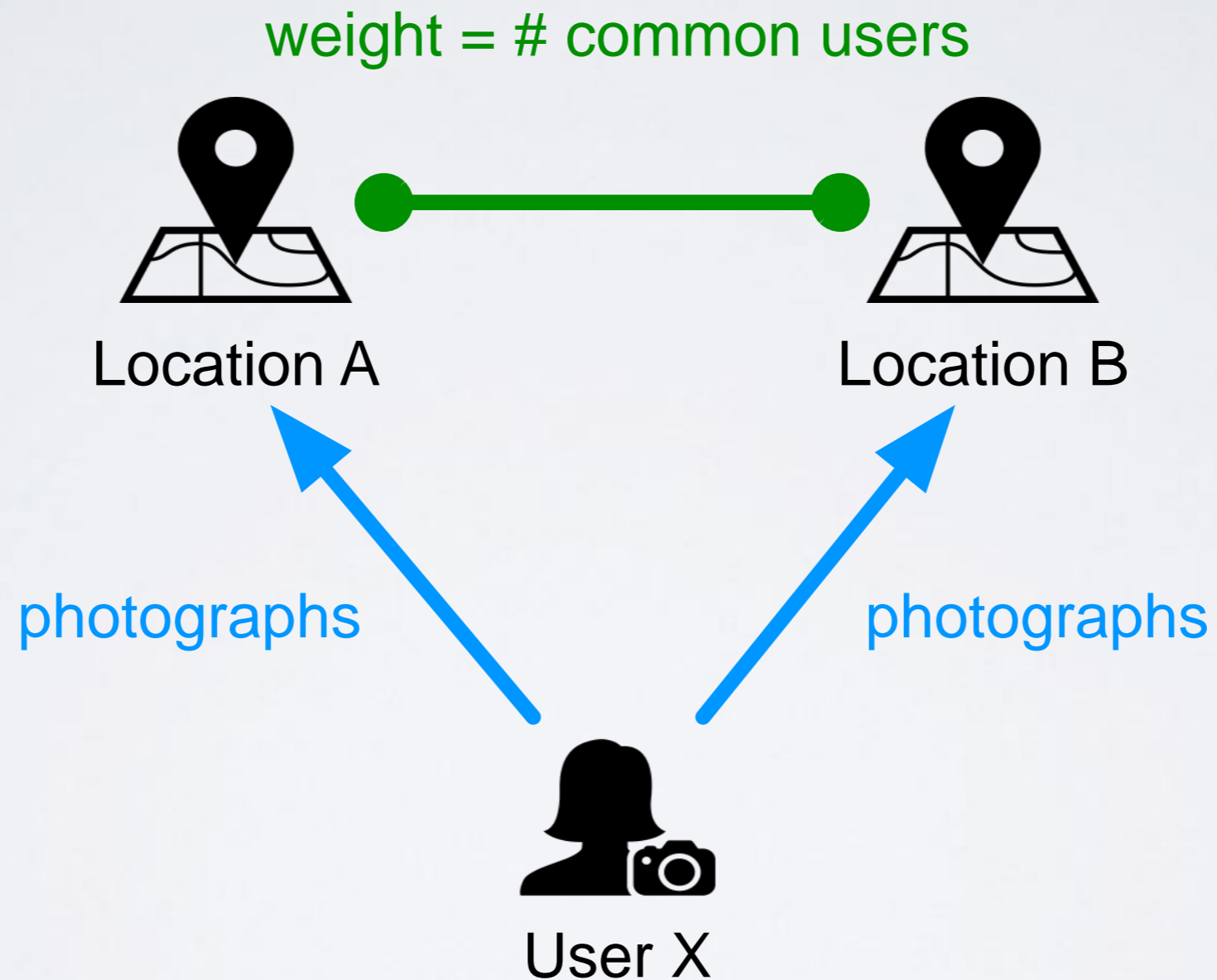


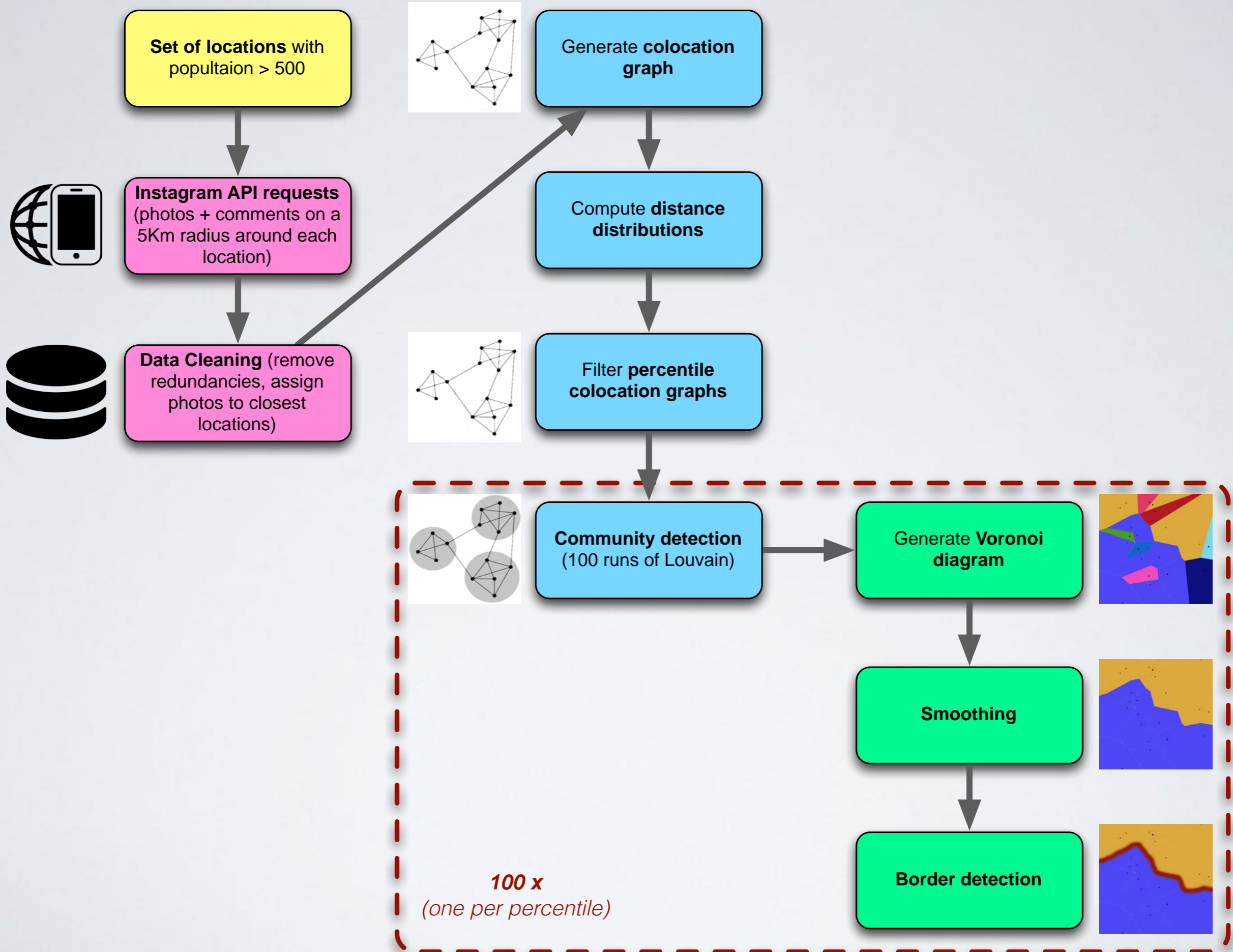
“COMMUNITY” DETECTION

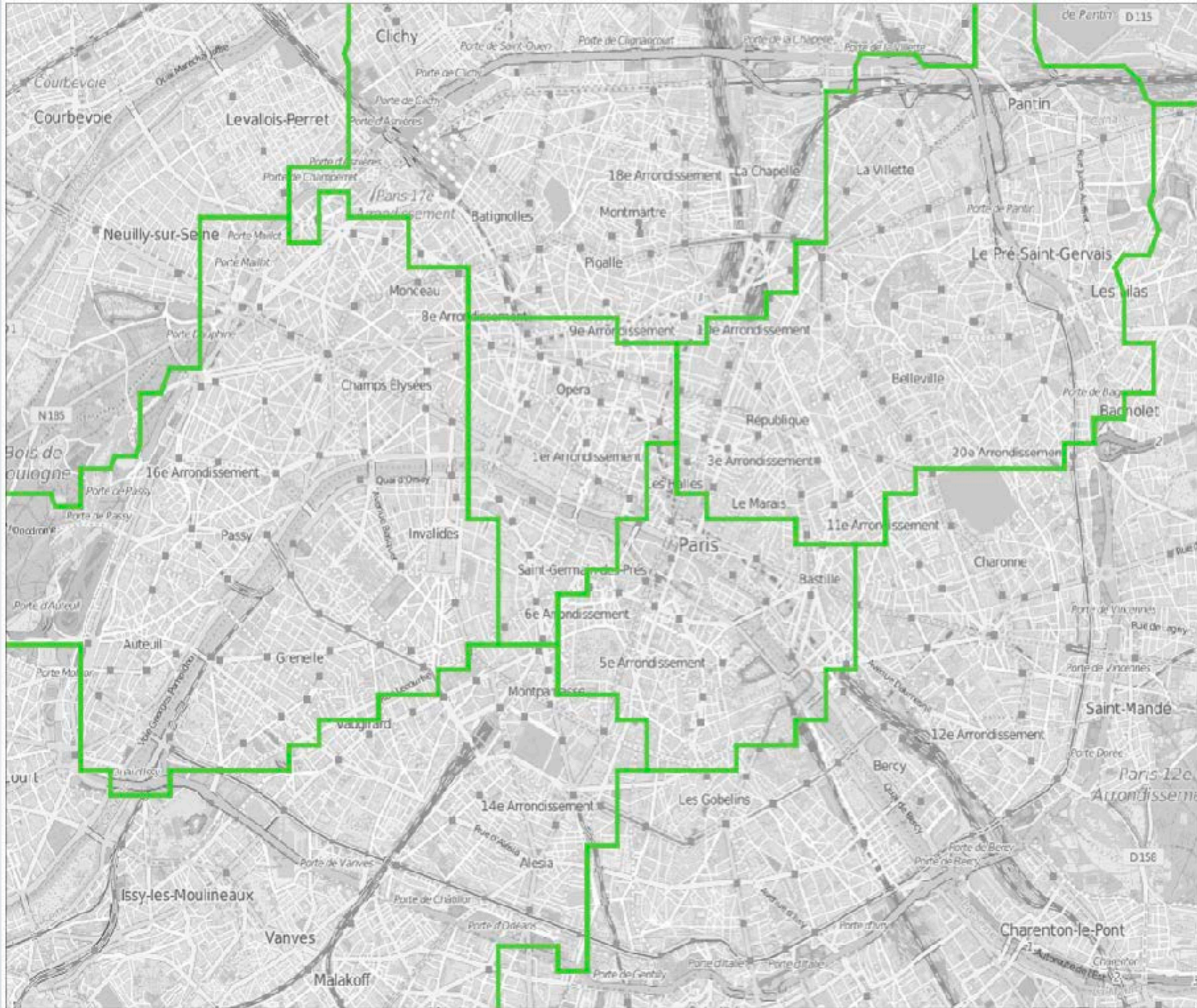
- **Normalize networks** with configuration model (avoid size effects)
- **Community detection** 100 times with Louvain algorithm (non-deterministic)
- **Force two communities** (optional extra step)
- **Detect borders** on Voronoi surface with weights (percentage of occurrences on Louvain runs)

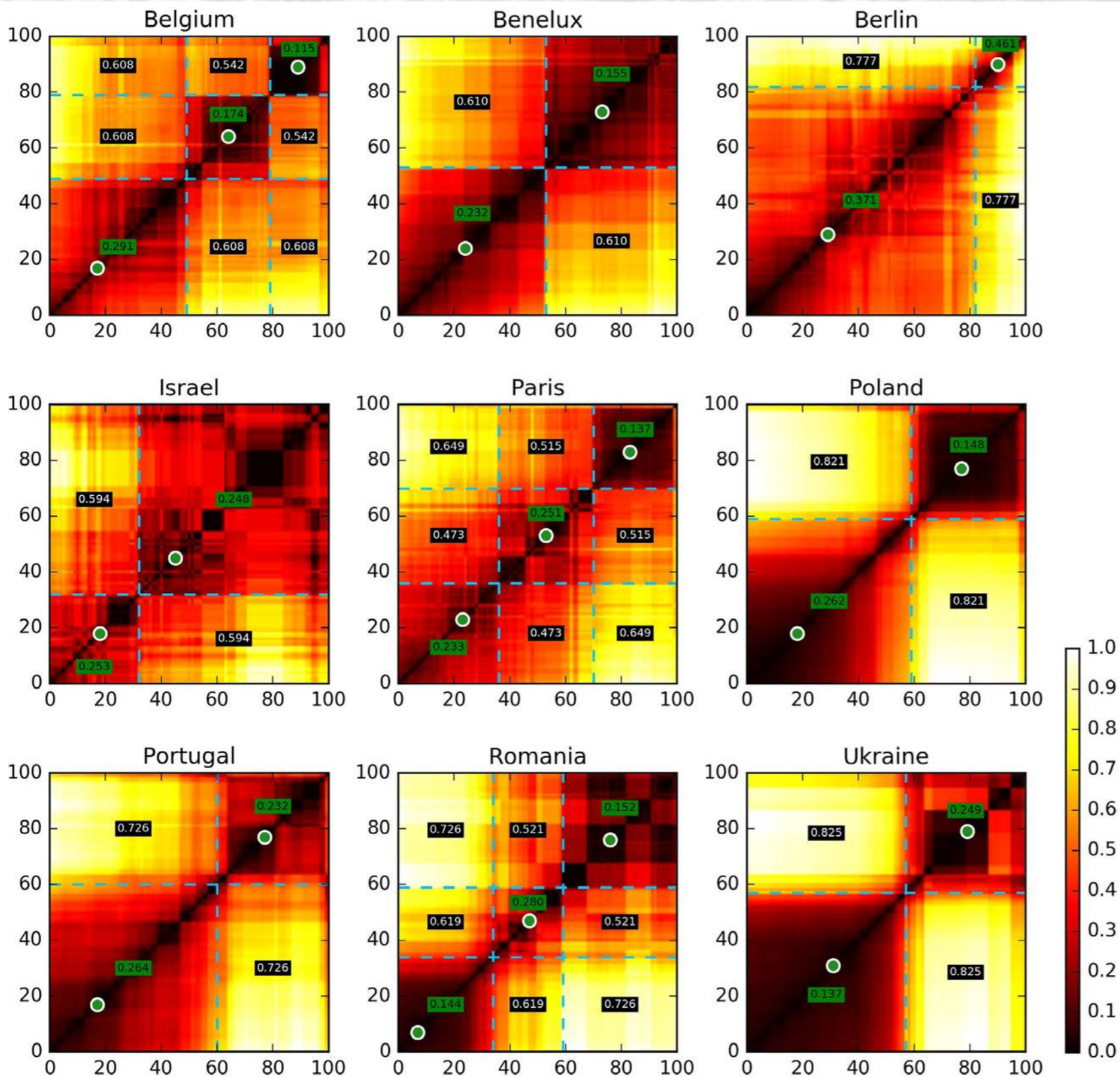


COLOCATION NETWORK









$$\mu^P(i, j) = \begin{cases} 1, & \text{if } \exists X \in P \text{ such that } i, j \in X \\ 0, & \text{otherwise} \end{cases}$$

$$\delta(V, P_s, P_{s'}) = \frac{|\{(i, j) \in V^2, i \neq j, \mu^{P_s}(i, j) = \mu^{P_{s'}}(i, j)\}|}{\binom{|V|}{2}}$$

Figure 1. Scale dissimilarity heat maps. Dissimilarity values are normalized per region to a $[0, 1]$ scale. Lighter colors represent higher dissimilarity. Pure black (0.0) corresponds to a perfect match, bright yellow (1.0) to the maximum dissimilarity found for the region. Dashed blue lines indicate the discontinuities identified by the breakpoint detection algorithm and, accordingly, natural scales; green dots represent the prototypical scale for each natural scale interval. The mean absolute dissimilarity value per pair of intervals is shown. A value in a green background corresponds to an internal mean dissimilarity (the interval is being compared to itself); a black background indicates a mean dissimilarity between different intervals.

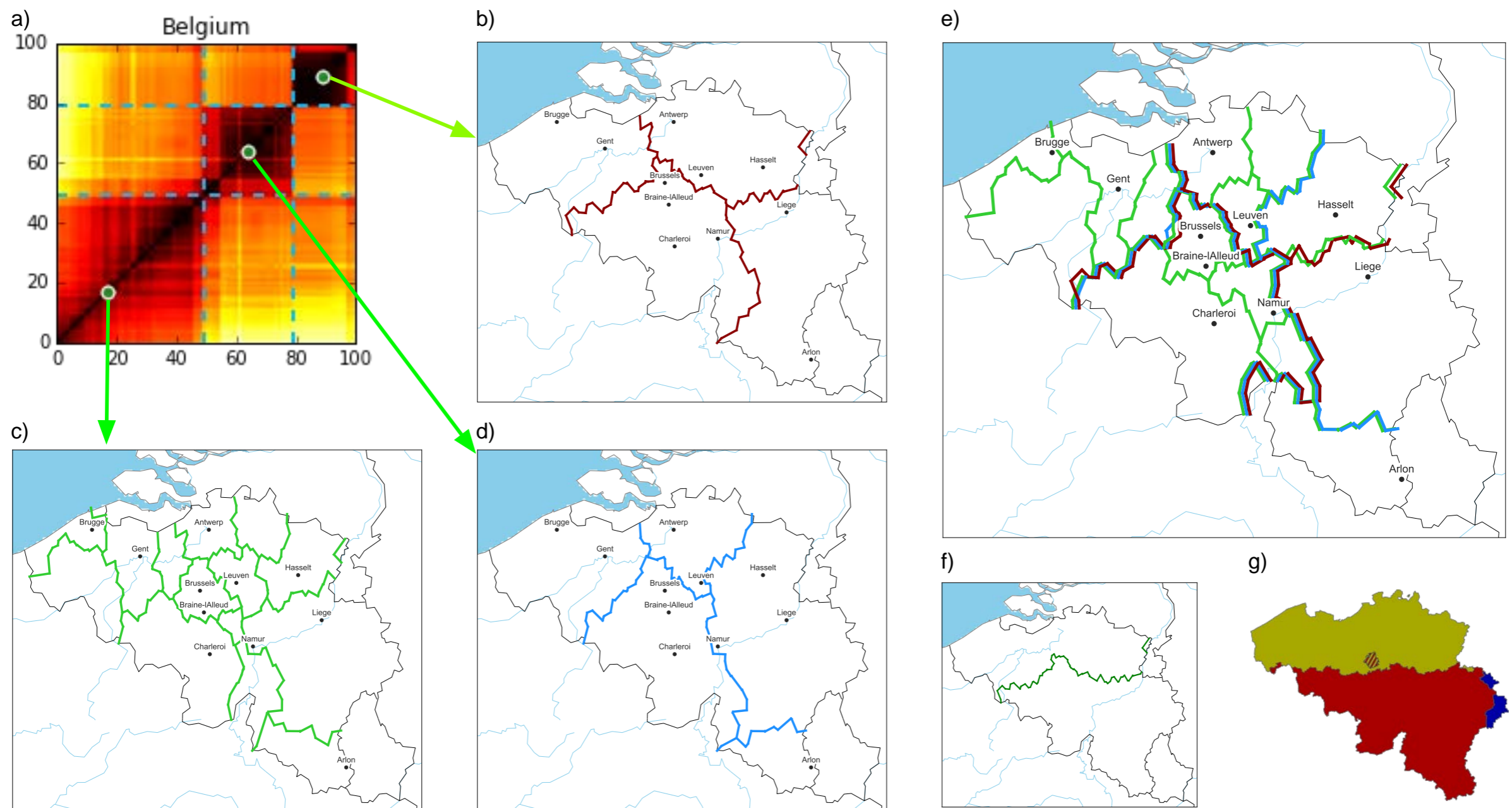
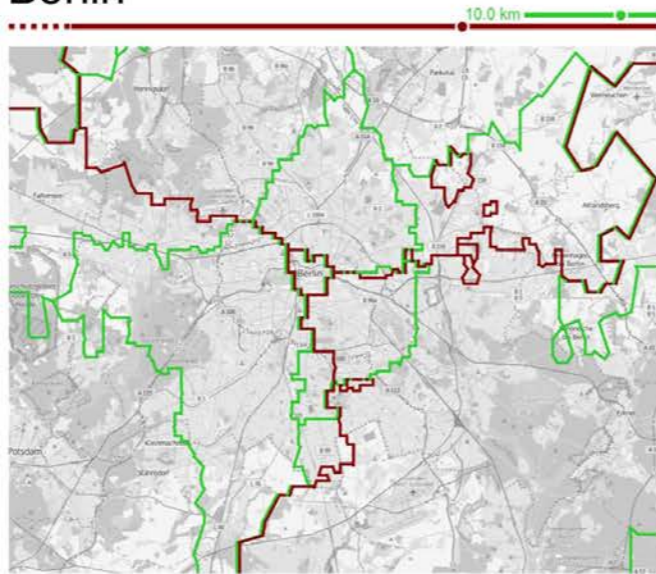


Fig. 2. *Belgium borders at different scales.* a) Heat map extracted from figure 1; b) Borders for the long distance scale; c) Borders for the short distance scale; d) Borders for the middle distance scale; e) Multiscale borders; f) Borders based on optimal two community partition of the full graph; g) Language communities of Belgium.

Berlin



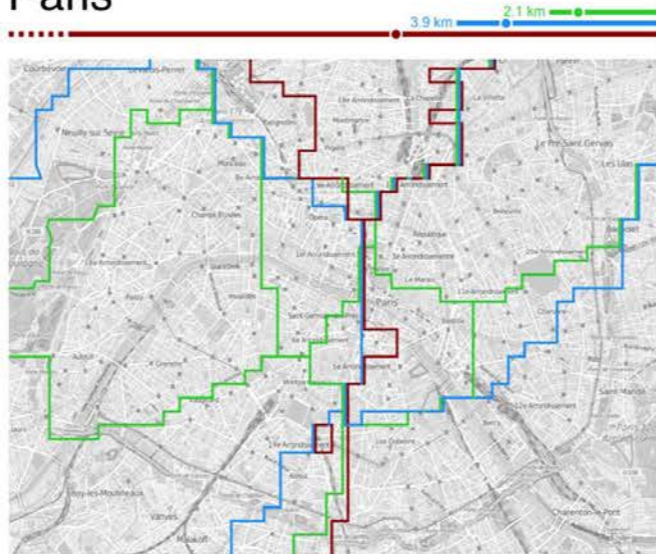
Benelux



Portugal



Paris



Poland



Israel



Ukraine



Romania

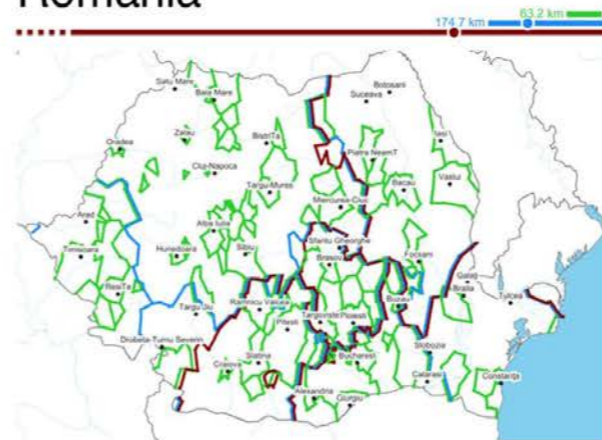


Figure 3. Several multi-scale maps. Green corresponds to the smallest natural scale, blue to the middle (if it exists) and red to the largest. All maps were generated by the authors using the Basemap Matplotlib Toolkit

